NUTRIENT CYCLING OF POTASSIUM IN THE CRITICAL ZONE OVER PERIODS OF CHANGING LAND USE

by

PETER STEINER

(Under the Direction of Paul Schroeder)

ABSTRACT

Potassium (K^+) is a macronutrient essential for plant growth which is derived from mineralogical sources. Well-established deep rooting profiles govern the nutrient cycling of K^+, yet past research has demonstrated that rooting profiles are not reestablished for over eighty years following land use change. This research investigates consequences for K^+ cycling dynamics after changes in land use by comparing the effects of the hardwood *Acer rubrum* on soil exchangeable potassium (EK) and clay mineralogy against the effects of the pine *Pinus taeda*. Both species had similar effects on EK, but *A. rubrum* imparted structural changes to the clay minerals which were not observed after the growth of *P. taeda*. These findings demonstrate that different chemical pathways may be used by various tree species as part of their K^+ uptake strategies, contributing to changing nutrient cycling dynamics over periods of changing land use.

INDEX WORDS: Calhoun Critical Zone Observatory, Soil science, Clay mineralogy, Biogeochemistry, Potassium, Exchangeable potassium, Nutrient cycling, Soil K cycle, Land use, *Acer rubrum*, *Pinus taeda*, X-ray diffraction

NUTRIENT CYCLING OF POTASSIUM IN THE CRITICAL ZONE OVER PERIODS OF CHANGING LAND USE

by

PETER STEINER

BA, DePauw University, 2017

A Thesis Submitted to the Graduate Faculty of The University of Georgia in Partial Fulfillment of the Requirements for the Degree

MASTER OF SCIENCE

ATHENS, GEORGIA

2021

NUTRIENT CYCLING OF POTASSIUM IN THE CRITICAL ZONE OVER PERIODS OF CHANGING LAND USE

by

PETER STEINER

Major Professor:	Paul Schroeder
Committee:	Daniel Markewitz
	Aaron Thompson

Electronic Version Approved:

Ron Walcott
Vice Provost for Graduate Education and Dean of the Graduate School
The University of Georgia
May 2021

ACKNOWLEDGEMENTS

This thesis is the product of interdisciplinary collaboration and required the guidance, assistance, and feedback of people from across varied disciplines of science. My thanks go out to all the individuals with which I discussed my project or who assisted in any way, but several names stand out for their exceptional assistance. First and foremost are my committee members for sticking with me on this unusually lengthy four-year research cycle for a Master's objective: Dr. Paul Schroeder, Dr. Daniel Markewitz, and Dr. Aaron Thompson. In addition to fulfilling your duties in providing feedback and guidance, you remained approachable and encouraging all the way to the end. Additional thanks go to Dr. Adam Milewski, who served on an earlier version of my committee and remained invested in my research to the end.

Special thanks to greenhouse manager Suzzanne Tate for upkeep of my growth experiments over the course of two summers in the Whitehall Forest greenhouse facilities and for discussions about my project. The unfamiliar territory of greenhouse work and biological specimens became far more manageable for a geologist like myself with her experience as a greenhouse manager to guide me. A huge thanks to both of my parents for their support and constant discussions with me about my project. Their background as microbiologists helped me consider more of the interdisciplinary angles and they were always ready to assist me whether I needed an extra hand collecting seeds from the wild or ferrying supplies between the cities of Atlanta and Athens. Science is not a solo endeavor, and this is especially true of interdisciplinary research. My sincerest thanks to all of the people named above and the many more I could not address in this space: you are the reason I am here.

TABLE OF CONTENTS

Page

APPENDICES

1. INTRODUCTION

1.1. The Soil K Cycle

Potassium (K^+) has been described as "the only univalent cation that is generally indispensable for all living organisms" (Evans and Sorger, 1966). In plants, K^+ is a macronutrient required for a variety of osmotic and enzymatic reactions. Deficiency in this nutrient results in chlorosis and necrosis of the plant (Evans and Sorger, 1966). Consequently, soil K^+ reserves are a major consideration for both agricultural and ecological applications.

Plants and soil microorganisms are able to mobilize K^+ from primary rock-forming minerals that contain it, such as K-feldspars (Andrist-Rangel et al., 2010; Lundström and Öhman, 1990) and micas (Bonneville et al., 2016; McMaster, 2012; Wallander and Wickman, 1999). However, special consideration must be made for secondary minerals such as clay minerals and weathered biotite. Once produced as weathering products, these phyllosilicates can store K^+ on interlayer and surface sites by charge attraction (Richter and Markewitz, 1995), turning them into a major reservoir of soil K^+ in weathered soils (Austin et al., 2018; Barré et al., 2007a; Shakeri and Abtahi, 2018).

Plant-mineral nutrient transfer is not a one-way interaction. Plants release the nutrients they have consumed through litterfall and throughfall, and K^+ ions released back into the soil from these processes can create or replenish K^+ reserves in otherwise depleted clay minerals. When deep-rooted trees take up subsurface K and cycle it to the near-surface in this way, the process is termed as "nutrient uplift" (Austin et al., 2018; Jobbágy and Jackson, 2004). The chemical changes plants impose on clay minerals can happen on timescales as short as weeks

(Barré et al., 2007b). Because the nutrient uptake and nutrient release from plants obey seasonality and the chemical changes can occur within mere weeks, even soils that are undergoing constant plant-driven K cycling may appear to have an annual net flux in K^+ that approaches zero even over multi-decadal experiments if measurements are taken annually (Barré et al., 2007a).

In addition to nutrient uplift, the root fibers of plants are able to mechanically and chemically alter surrounding minerals, which has been demonstrated through study of the rhizosphere. Mechanical alterations of the surrounding grains include the fracturing of grains adjacent to the root and the alignment and bending of sheet minerals such as micas in directions tangential to the roots, visible using scanning electron microscopy (April and Keller, 1990).

The primary means by which plants chemically modify the mineralogy of soils is by accelerating weathering through the release of low molecular weight organic acids (LMWOA), especially oxalic acid (Cama and Ganor, 2006; Fox and Comerford, 1990). Oxalic acid is a uniquely potent agent of chemical weathering, which has been demonstrated to be far more aggressive in dissolving mineral surfaces when compared against equivalent pH solutions of an inorganic acid such as hydrochloric acid (McMaster, 2012). Flow-through batch reactor experiments have supported the conclusion that the oxalate ion directly acts upon mineral surfaces to initiate oxalate-promoted dissolution mechanisms, rather than increasing dissolution rates through oxalate-driven catalysis of proton-promoted dissolution mechanisms (Cama and Ganor, 2006). The direct action of the oxalate ion upon mineral surfaces is thus responsible for its increased ability to weather minerals when compared against inorganic acids and even other LMWOA. However, certain organic ligands from plants may be capable of producing alternative effects, such as enhancing the crystallinity of kaolin group clay minerals in immediate

proximity to plant roots, though alternative explanations may exist for this observed phenomenon within the rhizosphere (April and Keller, 1990).

Plants do not act alone in the processes of nutrient uptake and organic acid production. Upwards of 80% of plants associate with mycorrhizal fungi that interface with plant roots via dendritic hyphal networks (endomycorrhiza). Other mycorrhizal fungi form sheaths around their root fibers (ectomycorrhiza). Both forms of mycorrhizal associations result in a mutualistic symbiosis in which the fungi receive carbohydrates from the plant in exchange for nutrients collected by its network of microscopic hyphae which provide a far greater contact area than the root fibers of the plant could achieve on their own (Woehrel and Light, 2017). A variety of mycorrhizal fungus species have been shown to enhance K^+ uptake by the associated plants (Wallander and Wickman, 1999; Yuan et al., 2004); however, enhancement may be controlled by plant nutrient demands and does not always occur (van Hees et al., 2006). Mycorrhizal fungi must accumulate K^+ efficiently, as they require this nutrient for their own processes as much as those of the host plant. These processes include the regulation of osmotic balance and of sporophore formation, leading to the greatest accumulations of K^+ within the sporocarps as opposed to the mycelium (typically an order of magnitude lower) or the surrounding rhizosphere (even lower yet) (Vinichuk et al., 2010).

Mycorrhizal fungi employ a variety of mechanisms to promote the release of K^+ from mineral sources. The release of LMWOA promotes K^+ release both through acid leaching and ligand-promoted chemical degradation (Cama and Ganor, 2006; Lian et al., 2008; McMaster, 2012). Furthermore, the mechanical action of the fungi on the minerals has been implicated as a source of physical weathering through direct contact, as supported by imagery captured using atomic force spectroscopy (Lian et al., 2008; McMaster, 2012) and helium-ion microscopy

(Lybrand et al., 2019). Furthermore, fungus-induced chemical weathering may beget additional mechanical weathering. In one study, structural strain upon the crystal lattice of biotite grains was found to be a product of Fe^{2+} oxidation by mycorrhizal fungi, which resulted in mechanical forcing of the K-bearing biotite grains (Bonneville et al., 2016).

The degree to which fungi actively seek out K-bearing minerals to colonize may depend on a number of factors such as plant nutrient demand, soil mineralogy, or fungal species. In one study, there was no observed preferential colonization of K-bearing minerals in nutrient-deficient soils even when P-bearing minerals showed preferential colonization (Rosenstock et al., 2016). Yet, a different study found increased carbon allocation by host plants and the associated mycorrhiza toward the roots and mycelia that were colonizing patches of K-feldspar as opposed to the ones colonizing nearby patches of quartz (Rosling et al., 2004). Regardless of what ultimately controls the fungal K^+ uptake, fungi appear to have the capability of regulating their behavior in response to their surroundings to deliberately induce weathering of nutrient sources they perceive as vital. This was demonstrated by a study in which the fungus *Aspergillus fumigatus* in the presence of K-bearing minerals showed an increased expression of genes governing the production of organic acids and carbonate (which would produce carbonic acid) when compared against a control without access to K-bearing minerals (Xiao et al., 2012). Though not in mycorrhizal association during that study, *A. fumigatus* has been used in mycorrhizal association with plants in other studies of mycorrhizal-promoted K^+ release in which increased K^+ uptake was noted (Lian et al., 2008). Thus, the upregulated genes identified in the genetic study are likely indicative of the response by *A. fumigatus* to a source of K^+ it requires, whether for its own processes or those of a host plant.

Plants and their fungal associations may be the primary drivers of the soil K cycle, but they are still beholden to external influences such as landscape evolution, including the ability of humans to modify landscapes drastically and rapidly. In the Calhoun Critical Zone Observatory (CCZO) located within Sumter National Forest (Union, SC), deforestation has imparted legacies upon the biotic component of a forest ecosystem even after 80 years of regeneration through a reduction in fine root density (Hauser et al., 2020) and an alteration of the microbial community's composition (Billings et al., 2018) when compared against minimally disturbed hardwood forests. In this same research area, differences were observed in the soil clay mineralogy of areas with differing land use histories, which was likewise linked to a loss of deep root density in deforested areas (Austin et al., 2018). Based on these related findings, one can conclude that the soil K cycle inherits a long-lasting belowground anthropogenic legacy once disturbed, even long after the forest seems to have visibly recovered aboveground.

1.2. Calhoun Critical Zone Observatory

The CCZO research area is an ideal site for studying the soil K cycle. The CCZO is an interdisciplinary research area set aside primarily on land that had formerly been severely degraded by large-scale erosion initiated by various agricultural practices in place from the 1700s up until the 1930s (Coughlan et al., 2017). Historical events had a major impact on land management during this time period. Slavery-based agriculture and later tenant-farming agriculture dominated this region. Both systems created circumstances where either the people in charge of day-to-day land use decisions (slave overseers) or working the land directly (tenant farmers) had no motivation to maintain the land for long-term use, because the land did not belong to these individuals in the first place. The actual land owners during these periods often

viewed the purchase of land not as a permanent investment, but as a momentary replenishment of an expendable commodity that was expected to be worn out over time. These practices resulted in a high degree of erosive land use across the region that would become the CCZO (Trimble, 2008).

The implementation of alternative management strategies after this initial point of severe degradation offers an opportunity to research the effect of differing land use histories on biogeochemical processes. These restorative practices were initiated during the 1930s across the region as a series of projects by the Civilian Conservation Corps (CCC), which coincided with a shift in perceptions of land sustainability and the implementation of sustainable land use strategies in land that was still owned and operated agriculturally, reducing erosive practices across the region (Trimble, 2008). Researchers attempting to compare different land use histories have generally grouped plots of land in the CCZO according to three main land use histories: minimally disturbed hardwood forest (no record of agriculture and evidence of >120 years without any), regenerating pine forest (degraded but then abandoned and allowed to recover), and cultivated (ongoing agricultural practices) (Austin et al., 2020; Austin et al., 2018; Billings et al., 2018; Hauser et al., 2020).

A variety of hardwood tree species (e.g., *Carya sp., Quercus sp.*) dominate the CCZO lands that researchers have described as minimally disturbed, whereas the regenerated plots are dominated by loblolly pines *(Pinus taeda* L.*)* (Billings et al., 2018). The dense pine cover in the regenerated plots gives the surface appearance that the land has recovered to a pre-agricultural state, but much research has been directed at testing the hypothesis that this landsurface appearance represents an "obscuring" of changed belowground biogeochemical processes, rather than restoration of pre-agricultural conditions (Austin et al., 2018; Billings et al., 2018). Both

microbial (Billings et al., 2018) and mineralogical (Austin et al., 2018) evidence support the conclusion that the regenerated plots have not restored soil nutrient cycles to the conditions observed in the minimally disturbed reference plots, which has been linked in part to a loss of deep root density.

Pines are among the minority of tree species that form ectomycorrhizal associations with fungi rather than endomycorrhizal associations (Woehrel and Light, 2017). Thus, different microbially-promoted nutrient cycling processes might have been established as the plots regenerated through ecological succession became dominated by *Pinus taeda*. Overall, the difference in species composition of these plots and legacy of persistent changes to microbial communities and mineralogy present an ideal opportunity to investigate how plants and their mycorrhizal fungi interact with soil minerals in a soil K cycle.

Furthermore, previous research in the CCZO has demonstrated that the plant communities of this ecosystem possess some ability to replenish soil potassium reserves over long-term growth, with only a small depletion in exchangeable soil potassium and a lack of depletion in non-exchangeable potassium (NEK) over the course of a three-decade study (Markewitz and Richter, 2000). These observations imply that the soil K cycle of biological uptake and renewal or replenishment to the soil minerals is ongoing and prominent in this research area. This precedent further reinforces the value of the CCZO for research related to the soil K cycle.

1.3. Hypothesis

Across the CCZO, soil nutrient cycles have not been restored to hardwood-dominated late-sucessional conditions even upon the reforestation of the land by pine-dominated forest

(Austin et al., 2018; Billings et al., 2018), I hypothesize that pine trees and their associated mycorrhizal communities utilize different minerals as their principal source of K^+ than the minerals used by hardwoods and their mycorrhizal communities for their principal sources of K^+. Because the changed soil nutrient cycling dynamics in the different plots of the CCZO have been interpreted as a consequence of the loss of deep root density, I further hypothesize that the pine trees are more able than hardwood tree species to obtain K^+ from minerals found in the upper soil horizons, which are for the most part clay minerals. The different soil nutrient cycles found in hardwood forests with deep root profiles could be interpreted under this hypothesis as the presence of nutrient flow uptake dynamics which also include primary rock-forming minerals found at greater depth in soils that have fully established rooting profiles.

Considering the effect of primary minerals deeper in the soil profile as a potential source of K^+ is important since there is clear evidence that such primary minerals (i.e., feldspars) can contribute K^+ to plant nutrition (Andrist-Rangel et al., 2006). Investigating specific mineralogical sources of soil K will provide important insight into long-term K availability (Markewitz and Richter, 2000).

Testing this hypothesis requires sampling of soil profiles beyond the depths that are typically studied. Researchers have remarked in recent years upon the notable lack of studies which investigate long-term soil processes below the upper 30 centimeters of the soil profile (Mobley et al., 2015). Research to test this hypothesis is of value not just in differentiating the changes in soil nutrient dynamics over the course of ecological succession and landscape evolution, but also in expanding our understanding of soil processes at depths beyond the upper 30 cm of soil. Understanding soil and the processes that govern it not merely in this upper portion of the profile, but rather throughout the entire soil profile from the surface to the bedrock,

will be crucial to safeguarding our soils against potential threats that can have major financial repercussions for government and individuals, such as erosion and biodiversity loss among others (Banwart et al., 2012).

In this research, red maple trees (*Acer rubrum*) will be used as a representative of hardwood trees with potential for endomycorrhizal communities, as opposed to loblolly pine trees (*Pinus taeda*) as representatives of pine trees with potential for ectomycorrhizal communities. Neither tree should be considered representative of all members of these categories, but rather as one representative which can be used as a point of comparison between these categories for this K-cycling study. The hypothesis of differential mineral use by maples as opposed to pines is hereby tested using a small-scale proxy for landscape-scale nutrient cycling as past researchers have done (Barré et al., 2007b; Rosling et al., 2004; Wallander and Wickman, 1999). My hypothesis is tested with a greenhouse growth experiment followed by two separate but complementary forms of analysis: exchangeable potassium (EK) extraction and powder X-ray diffraction (XRD) of the clay fraction.

2. METHODS

2.1. Pilot Study

An initial pilot study was conducted to assess the viability of a 90-day greenhouse growth experiment in producing measurable changes in exchangeable potassium (EK) concentration among different soil samples collected from areas proximal to the CCZO. Sample materials were collected from a quarry owned and operated by Hanson Aggregates in Clinton, SC located immediately outside the protected boundaries of the Sumter National Forest. This quarry provided sampling access to a depth profile representative of materials in the CCZO from the soil surface down to the bedrock. The bedrock quarried at this site is best described as a gneiss which approaches migmatite-grade metamorphism and contains aplitic dikes and trace amounts of epidote (Figure 1). Three sample materials were collected from this site (designated Q1), and are described below using Munsell colors.

Sample Q1-B is a 10R 5/4 argillic Bt horizon collected from the quarry overburden, which would have been located at a depth of a few to several meters beneath a hardwood forest prior to quarry excavation. Sample Q1-C is a 10YR 4/2 Cr horizon collected from immediately above the quarry walls, where the deepest soil lies in direct contact with the bedrock. Sample Q1-R consists of bedrock collected directly from the quarry floor, which was later pulverized in a Bico Chipmunk jaw crusher (Gilson Company, Inc., Columbus, OH) and Bico pulverizer (Gilson Company, Inc., Columbus, OH) into a substrate of coarse sand derived from R horizon.

To normalize water flow between these texturally diverse substrates during the greenhouse experiment, 20% silica sand (Rollo Pond Filter Sand, Atlanta Sand & Supply

Company, Macon, GA) by mass was added to each of the substrates. Silica sand was used because it is K-free and could be assumed as chemically inert during the experiment.

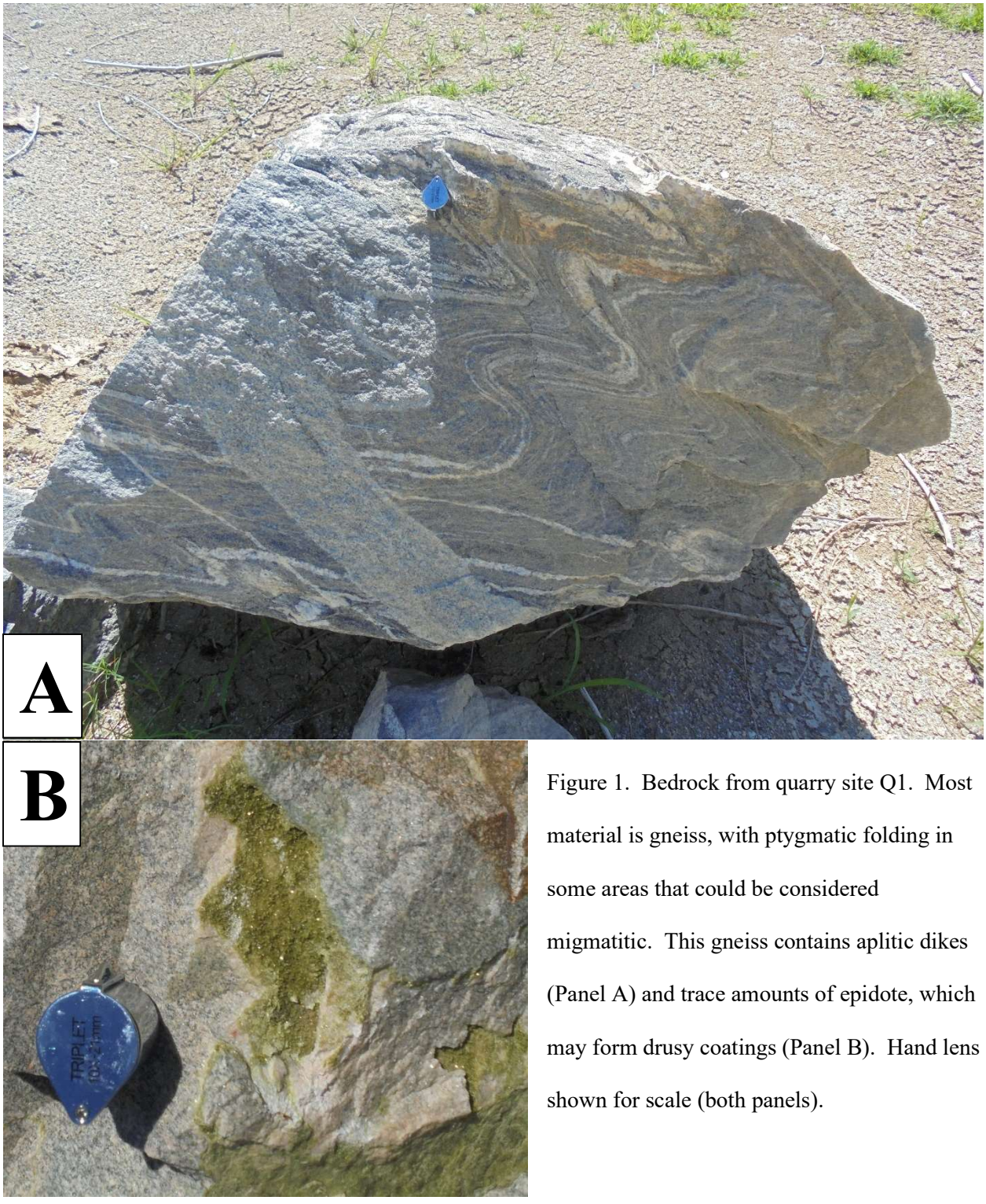

Figure 1. Bedrock from quarry site Q1. Most material is gneiss, with ptygmatic folding in some areas that could be considered migmatitic. This gneiss contains aplitic dikes (Panel A) and trace amounts of epidote, which may form drusy coatings (Panel B). Hand lens shown for scale (both panels).

Acer rubrum and *Pinus taeda* seeds were collected from north-central Georgia, United States and sown directly into 30-cm deep growth wells filled with these substrates, with ten replicates (Figure 2). To prevent loss of substrate out of the base of growing pots during the experiment, soil retainment mesh (Vigoro weed block film, Home Depot, Atlanta, GA) was cut into 10 cm x 10 cm squares and fixed in place around the exterior of the growth wells using rubber bands. Samples were watered twice daily using deionized water and maintained in the greenhouse facilities at the University of Georgia Whitehall Forest facility (Athens, GA) during the summer of 2019.

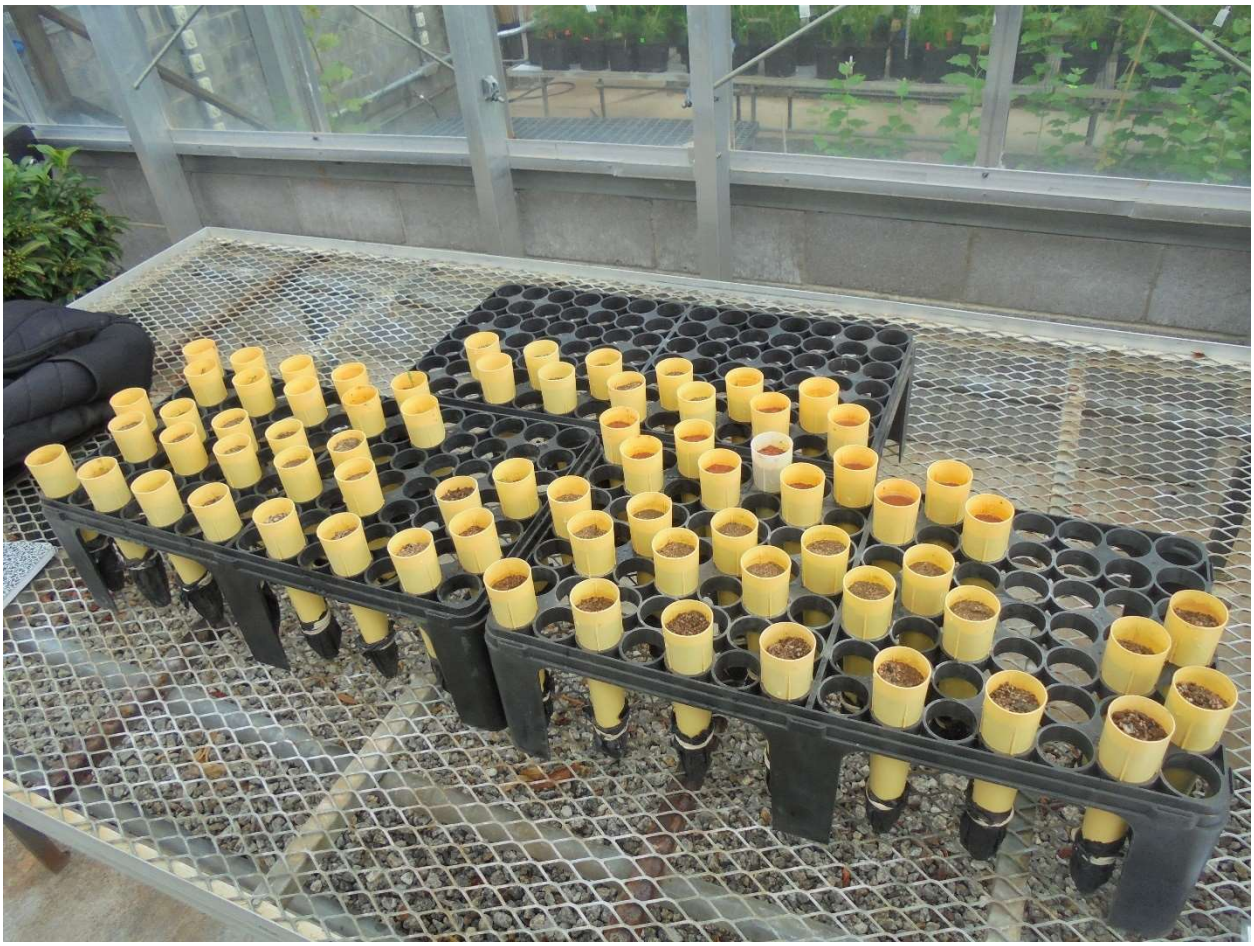

Figure 2. Experimental setup used in the pilot study with seeds sown directly into substrate.

This initial experiment faced several challenges. *Pinus taeda* seeds failed to sprout, and that component of the experiment was terminated after one month. Among the seeds of *Acer rubrum,* only a few of the seeds sprouted, resulting in a low number of replicates. To begin amending the experimental design for a more successful attempt in the following summer, additional samples of live seedlings (estimated at one year in age) were collected from the same site in north-central Georgia as the seeds. These seedlings were placed in additional growth pots with the same substrates, in order to observe how the seedlings might have fared had they germinated and sprouted successfully (Figure 3). Drought stress was observed in these plants within the first month. In an attempt to remedy this condition with readily-available materials, plastic cups were arranged beneath the growth wells to collect the draining water and act as reservoirs that would soak the bottom of the growth well and retard moisture loss. This was largely successful among the maples, but the pines died in large quantities over the month following this addition. This high mortality was likely because conditions then became too wet for the drought-tolerant pines.

Figure 3. Pilot study supplemented with grown seedlings, estimated one year in age.

After a 90-day period from being sown, the maple seedlings which had been successfully raised from seed were collected for analysis. The materials collected from these wells were extracted with ammonium acetate to quantify exchangeable potassium abundance via atomic absorption (AA) spectroscopy (Page, 1982). These procedures are described in greater detail under the subsection *Exchangeable Potassium*. The number of viable samples was insufficient for meaningful statistical analysis, but the data demonstrated a noticeable difference between the few surviving maples and control wells which had no seeds sown in them, providing proof of concept that this experimental design could be modified to provide meaningful data.

Several complications faced in this pilot study were noted, and the experimental design for summer 2020 was amended accordingly. The failure of the samples to germinate could be amended by a more rigorous germination procedure using an idealized germination medium, such as sphagnum peat moss, and an initial period of protected growth. The drought stress could be prevented by installing reservoirs to capture draining water and retard moisture loss from the onset of the growth period. The death of pines under these moister conditions could be prevented by a reduction from watering twice each day to watering once each day. An overall larger number of surviving samples would result in sufficient replicates for meaningful statistical analysis.

Furthermore, the growth wells proved to hold far more soil material than the seedlings could penetrate with their roots over 90 days of growth from seed, and so any chemical changes the plant might cause were difficult to detect. This could be amended by using growing pots of a much smaller volume. The soil retention mesh also began to fall off the wells as sunlight degraded the rubber bands holding it in place, allowing soil loss near the end of the experiment. This could be prevented by instead placing the soil retention mesh inside the receptacles and allowing the weight of the soil to hold it down over the drainage holes, rather than affixing the mesh to the outside with rubber bands. Lastly, water flow was not normalized despite the addition of 20% silica sand (and may have contributed to the death of the pines in the argillic Q1-B material with its high moisture retention), so a higher percentage of the chemically-inert silica sand would be necessary to achieve this goal. Over the course of 2020, a modified version of this pilot experiment was conducted, using these changes to improve the quality and quantity of collected data. The methods of this amended experiment and the analyses used to interpret it are covered in the following subsections of this methodology.

2.2. Sample Selection

Setup for a more rigorous growth experiment during the 2020 growing season began with the selection and preparation of additional soil substrates associated with the CCZO. A series of pits were excavated with a backhoe from October to December of 2016 as part of a collaborative effort of CCZO researchers to investigate soil horizons at a range of depths up to a few meters in various research watersheds (designated R1-R8). Soil samples from these regions across the CCZO were collected and a portion stored at the University of Georgia (UGA). Soil samples from from 200-700 cm depth from the available materials at UGA were selected and used in the experiment in addition to Q1-B, Q1-C, and Q1-R.

Sample R1-C3-B is a 2.5YR 5/4 Bt horizon, similar in appearance to Q1-B, collected at a depth range of 200-300 cm from beneath cultivated land. Sample R1-C3-C is a 5YR 5/4 BC horizon collected at a depth range of 400-500 cm from the same excavation site as R1-C3-B. Sample R7-P2-B is a 2.5YR 4/3 Bt horizon collected at a depth range of 300-400 cm from beneath pine forest. Sample R7-P2-C is a 5YR 5/3 C horizon collected at a depth of 600-700 cm from the same excavation site as R7-P2-B. Sample R8-P1-C is a 10YR 4/2 C horizon collected at a depth range of 400-500 cm from beneath pine forest. Sample R8-H1-C is a 10YR 5/2 C horizon collected at a depth range of 400-500 cm from beneath hardwood forest.

In summary, samples came from five total sites: CCZO excavation pits R1-C3, R7-P2, R8-P1, and R8-H1 and the CCZO-proximal quarry site Q1. Together, these samples represented a considerable range of the conditions found in and around the mesic hardwood environment of the CCZO research area. These conditions included depths ranging from near-surface (R1-C3-B) to near-bedrock (Q1-C) or bedrock-equivalent (Q1-R) and land use histories ranging from

continuous agriculture (R1-C3 samples) to hardwood forest undisturbed within recorded history (R8-H1-C). These samples also represented a gradient in bulk soil K_2O from 0.17 weight % (R1-C3-B) to 3.98 weight % (R8-H1-C) based on the findings of prior research (Austin and Schroeder, 2019).

Based on the difficulties faced during the pilot experiment, the fraction of chemically inert silica sand (Rollo Pond Filter Sand, Atlanta Sand & Supply Company, Macon, GA) added to each sample to homogenize the hydrologic drainage during watering was increased from 20% to 50%. Furthermore, the measurements of sample material and silica sand were taken by volume rather than mass, as this was deemed more appropriate for homogenizing hydrologic conditions (volume being a measurement of space and therefore more representative of the spacing between particles which would be achieved). These materials were prepared March 31, 2020 and then stored until the biological components of the experiment were ready.

2.3. Growth Experiment

Seeds were collected from north-central Georgia, United States on February 17, 2020 (*Pinus taeda*) and April 7, 2020 (*Acer rubrum*) upon naturally falling from the parent trees and allowing for minimal contact time with the ground. *Acer rubrum* seeds were stored in dry conditions at room temperature (21° C) and *Pinus taeda* seeds were maintained at 4° C for cold stratification. Seed stratification consisted of placing seeds at 4° C inside a Ziploc® bag with a wet paper towel until visible signs of germination were present. Seeds were then sown (3 to 4 mm depth) into a germination tray containing premoistened Canadian sphagnum (Sun Gro Horticulture Distribution, Inc., Agawan, MA, catalogue No. F1971) on May 3, 2020 (*Acer rubrum*) (Figure 4) and June 9, 2020 (*Pinus taeda*). Seeds were watered with deionized water.

Germination trays were maintained under sheltered environmental conditions (i.e. shielded from rainfall) (Figure 5) for 18-21 days until the second set of permanent leaves had started to emerge for *Acer rubrum* and until the seedlings had the first tuft of needles for *Pinus taeda*.

Figure 4. Germination tray with maple seeds on 5/2/20.

Figure 5. Maple seedlings on 5/17/20 with the first set of permanent leaves, one week prior to transplantation from germination medium to experimental substrate. A second set of permanent leaves was added in the final week.

Seedlings were then transplanted to the CCZO soil samples (Figure 6 and Figure 7). To eliminate transfer of sphagnum, each seedling was carefully removed from the germination tray and the roots were gently washed with deionized water with the aid of a watering bottle until no visible sphagnum was observed clinging to root fibers. *Acer rubrum* roots were approximately 1 cm in length upon transplantation and *Pinus taeda* seedlings possessed tap roots approximately 1-3 cm in length. Seedlings were transferred for each soil sample onto 72-cell seed starter receptacles (Plantation Products, LLC, Norton, MA). To prevent the loss of sample material during watering, Vigoro weed block film (Home Depot, Atlanta, GA) cut into sections measuring 2 cm x 2 cm was placed at the bottom of each receptacle. Then, 40 mL of each soil sample was added to each receptacle. Transplanted seedlings were closely monitored under sheltered environmental conditions for 12 more days to ensure they survived transplantation-induced stress before transfer to and maintenance in a greenhouse facility (University of Georgia Whitehall Forest facility, Athens, GA). To maintain moisture, 60 mL polyethylene vessels were placed below each growth receptacle to act as reservoirs.

Figure 6. Maple seedlings on 5/24/20 immediately following transplantation into experimental substrates. Overall arrangement (Panel A) and close-up (Panel B) shown.

Figure 7. Pine seedlings immediately following transplantation on 6/30/20 into experimental substrates.

Samples were maintained for 90 days in the greenhouse facility (Figure 8 and Figure 9) from the day of transplantation until the soil samples were collected for EK extraction and XRD analysis. The plants were watered with deionized water once (*Pinus taeda*) or twice (*Acer rubrum*) each day in accordance with the degree of drought tolerance or flood tolerance of the species, respectively. No fertilizer was added to any treatment. Enough seedlings survived the germination and initial growth period to allow eight samples of *Acer rubrum* for each selected test material and six samples of *Pinus taeda*. However, limited quantities of *Pinus taeda* surviving this initial growth period limited the experiment to testing only six of the nine soil

samples even at this slightly reduced number of replicates. Seven controls (substrate with no sown plants) of each test material were also maintained and watered daily in the greenhouse.

Figure 8. Maple seedlings on 7/12/20 after 30 days of greenhouse growth. Overall arrangement (Panel A) and close-up (Panel B) shown.

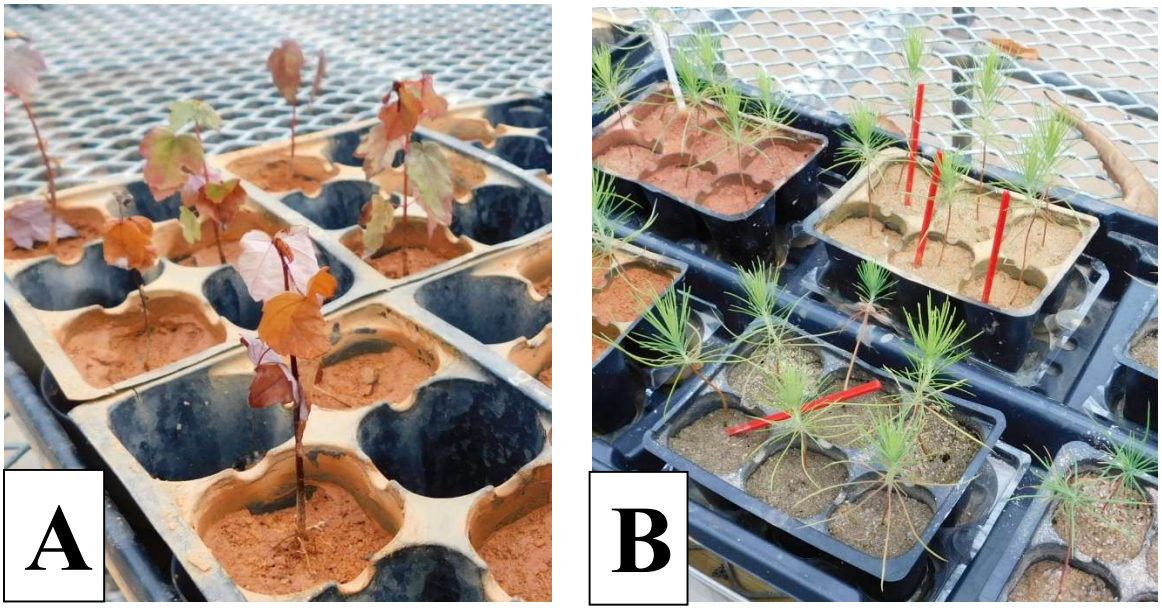

Figure 9. Maple seedlings on 8/9/20 (Panel A) after 58 days of growth and pine seedlings on 9/20/20 (Panel B) after 60 days of growth. Note that some necrosis and dropped leaves are present among the maples, but this is not necessarily due to potassium deficiency as any number of stress factors can be responsible. Only a few organisms died despite this stress.

2.4. Exchangeable Potassium

Following the growth experiment, all samples were reduced to the five replicates with the healthiest plants. This was done to equalize the number of replicates among samples (some samples had replicates that died) and to ensure vigorous plant demand. These five replicates for each sample and an equal number of controls were analyzed using standard operating procedures for the extraction and quantification of exchangeable soil potassium following Page (1982).

In brief, 5 mL of sample material, measured by volume, was placed into a 50-mL centrifuge tube. The average mass of these 5 mL volumes for each sample was recorded for density calculation. Centrifuge tubes were then filled with 25 mL of 1.0 *N* NH_4OAc. Tubes were shaken for 20 minutes on a shaker tray and then centrifuged. The supernatant was decanted and the procedure was then repeated with an additional 25 mL of NH_4OAc. The two batches of

supernatant were combined into a single 50 mL extractant for analysis. The extractant was then analyzed for K using an AA spectrophotometer. The data were analyzed using Microsoft Excel and R.

2.5. Clay Fraction XRD Mineralogy

Prior to mineralogical analysis, replicates were composited and homogenized. Each of these composites was subsampled for 20g of material, which was prepared for XRD analysis following Austin et al. (2020, 2018). The subsample from each material was combined with 10% synthetic zincite by mass to act as an internal standard for the XRD. Flocculation of the clay fraction (defined as < 2 μm) was prevented by adding 100 mL of a dispersant in deionized water followed by dispersion with a Branson Sonifier Cell Disruptor 350 (Branson Sonic Power Company, Danbury, CT, United States). The sediment was reduced down to the silt fraction (defined as < 63 μm) through a sediment sieve and ultimately reduced to the clay fraction through centrifugation (Schroeder, 2018).

Due to the Na^+-rich nature of the dispersant, these clay fractions were considered Na^+-saturated following these treatments. In order to study the mobility of ions from exchangeable sites in the clay minerals, these clay fractions were split in half to undergo separate treatments of K^+-saturation and Mg^{2+}-saturation. Once reduced to the clay fraction by centrifugation, the dispersant was poured off and replaced by a solution of 1.0 M KCl (Fisher Chemical, Fairlawn, NJ, United States) for K^+-saturation and 0.1 M $MgCl_2$ (Acros, Morris Plains, NJ, United States) for Mg^{2+}-saturation. The sample material was agitated into suspension within these solutions for maximum exposure, then settled out by centrifugation and the solution renewed. This saturation process was repeated twice followed by two rinses in deionized water to remove excess solution.

This Na-saturated clay was suspended in deionized water as a slurry and pipetted onto petrographic slides which were dried overnight. The suspension was pipetted onto the slide with a volume intended to achieve an idealized infinite X-ray thickness (>10 mg/cm^2). These slides were then analyzed by XRD analysis using a Bruker Advance D8® X-ray diffractometer (Bruker, Karlsruhe, Germany) with Fe-filtered Co-Kα radiation (35 kV, 40 mA). XRD scans of the slides after air-drying overnight were followed with three subsequent scans taken after baking the slides at incrementally increased temperatures (110° C, 350° C, and 550° C). All XRD scans were taken from 2 to 45° 2θ using a step size of 0.01° 2θ and a scan speed of 0.1 s/step. Samples were prepared and run in triplicate. The data were recorded using a Bruker LynxEye® detector. The resulting diffractograms were analyzed using the analytical software DIFFRAC.EVA. Diffractogram peaks associated with the synthetic zincite internal standard were used to adjust the *x*-axis of the diffractograms to correct for displacement errors in samples that had experienced curling or peeling of the sedimented samples during heating.

2.6. SEM Imagery

In an attempt to better visualize the root fibers and their relationship with the surrounding mineral grains, clipped fine root fibers were mounted onto stubs, carbon-coated, and imaged using a scanning electron microscope (SEM). These images were collected as a supplement to the primary means of data acquisition discussed above. The SEM images were not used to inform interpretations and for this reason the images are not presented or discussed in the following chapter. Rather, a selection of these images is reproduced in Appendix C.

3. RESULTS

3.1. Exchangeable Potassium Abundance

Raw values of potassium detected by the AA spectrophotometer were averaged and corrected for density. Confidence intervals (CI 90%) for these averages were calculated and reported to provide a measure of the uncertainty. These values are reported in ppm EK concentration in Table 1, normalized to 5.0 g sample material.

The EK changes relative to control were evaluated as an increase, decrease, or no change a Welch two-sample *t*-test between each sample and the relevant control. The data were also used to run a two-way ANOVA to determine the influence on EK of soil sample, plant type (or control), and the interaction between plant type with soil sample. All terms were found to be statistically significant (soil sample: $F = 60.2$, $df = 8$, $p = 2.0 \times 10^{-16}$; plant type: $F = 10.4$, $df = 2$, $p = 8.15 \times 10^{-5}$; interaction: $F = 4.67$, $df = 13$, $p = 3.19 \times 10^{-6}$).

At a critical value of $\alpha = 0.10$, maple and pine growth did not cause a change in EK abundance large enough to resolve the difference between those samples and the controls of the respective material for the following samples: R1-C3-B, R8-P1-C, and Q1-B. In all other CCZO samples, mean EK changed relative to the controls. Changes in samples for R7-P2-B are statistically significant for only the maple seedlings ($p = 0.09$), but this statistic is contested by overlap in the CI 90% relative to the CI 90% for the control. For this reason, R7-P2-B is not considered to have changed.

Sample R1-C3-C demonstrated one of the most notable differences in EK between test samples and the relevant controls, with controls possessing an average of nearly five times the

EK of the samples containing maple seedlings (18.5 ± 3.2 ppm versus 4.4 ± 1.0 ppm). Sample R8-H1-C demonstrated another notable depletion of EK when comparing controls against the samples with maple seedlings (14.0 ± 1.9 ppm versus 9.9 ± 1.6 ppm).

R7-P2-C experienced a similar depletion in EK relative to the controls within the samples containing pine seedlings (17.4 ± 2.6 ppm versus 10.7 ± 2.0 ppm). Samples from R7-P2-C containing maple seedlings also averaged lower than the controls (12.0 ± 4.6 ppm versus 17.4 ppm ± 2.6 ppm), but $p > 0.10$ for maple seedlings versus controls. Consequently, this observation was deemed as no change.

Sample	Plant Type	Mean EK (ppm)	CI (90% CI)	Upper Bound (90% CI)	Lower Bound (90% CI)	EK Change	T-test
R1-C3-B	Control	9.6	5.0	14.6	4.6	Control	NA
	A. rubrum	4.3	3.1	7.5	1.2	None	$p = 0.18$
R1-C3-C	Control	18.5	3.2	21.8	15.3	Control	NA
	A. rubrum	4.4	1.0	5.4	3.3	Decrease	$p < 0.01$
R7-P2-B	Control	16.1	3.2	19.3	12.9	Control	NA
	A. rubrum	11.2	2.6	13.9	8.6	None	$p = 0.09$†
	P. taeda	13.5	2.2	15.7	11.3	None	$p = 0.30$
R7-P2-C	Control	17.4	2.6	20.0	14.8	Control	NA
	A. rubrum	12.0	4.6	16.6	7.4	None	$p = 0.14$
	P. taeda	10.7	2.0	12.7	8.6	Decrease	$p = 0.01$
R8-P1-C	Control	6.1	0.9	6.9	5.2	Control	NA
	A. rubrum	5.5	1.6	7.1	3.9	None	$p = 0.61$
	P. taeda	7.5	1.4	8.9	6.1	None	$p = 0.19$
R8-H1-C	Control	14.0	1.9	15.9	12.1	Control	NA
	A. rubrum	9.9	1.6	11.5	8.3	Decrease	$p = 0.03$
Q1-B	Control	30.5	2.0	32.5	28.5	Control	NA
	A. rubrum	31.4	6.5	37.9	24.9	None	$p = 0.83$
	P. taeda	36.6	5.4	42.0	31.2	None	$p = 0.14$
Q1-C	Control	16.7	1.2	17.9	15.5	Control	NA
	A. rubrum	18.2	0.4	18.6	17.9	Increase	$p = 0.10$
	P. taeda	26.3	2.5	28.8	23.7	Increase	$p < 0.01$
Q1-R	Control	6.0	0.8	6.8	5.2	Control	NA
	A. rubrum	8.5	1.1	9.7	7.4	Increase	$p = 0.02$
	P. taeda	6.6	1.0	7.6	5.5	None	$p = 0.49$

Table 1. Exchangeable potassium measurements with estimates of uncertainty (CI 90%), change, and *p*-values from supporting *t*-tests (Welch two-sample, log-normalized data). Maple samples for R7-P2-B are marked with a cross (†). This test group had $p < 0.10$, but overlaps in CI 90% with the control, so this sample was deemed as no change regardless.

In sample Q1-C, EK *increased* relative to the controls within the samples containing pine seedlings (16.7 ± 1.2 ppm versus 18.2 ± 0.4 ppm). Q1-R behaves similarly for samples with maple seedlings (6.0 ± 0.8 ppm in controls versus 8.5 ± 1.1 ppm in maple samples). However, this observation does not hold true for the pines, which are indistinguishable from the controls. Regardless, this creates a similarity in the observations made for Q1-C and Q1-R when compared against the other samples, because only Q1-C and Q1-R experienced an increase in EK whereas other samples experienced decreases or no change. The similarity in behavior between Q1-C and Q1-R may be reasonably expected; these samples were in immediate proximity and Q1-C would have been derived from the weathering of bedrock (Q1-R) at this site.

In summary, samples R1-C3-C, R7-P2-C, and R8-H1-C had lower EK than their respective controls regardless of plant species. By contrast, EK increased for samples Q1-C and Q1-R (with the exception of pines in Q1-R which could not be distinguished from controls). All other samples experienced no change in EK.

3.2. XRD Diffractogram Analysis

Using the Bruker analytical software DIFFRAC.EVA, the XRD patterns from multiple scans were plotted together for comparison. Three peaks were present in each diffractogram from $2\theta = 37^{o} – 42.5^{o}$. These peaks represented the internal standard of synthetic zincite added to each sample during preparation. These peaks were used to align diffractograms when *x*-axis shifts occurred due to displacement errors, but have little bearing on interpretation of the data. The peaks of interest are the low-angle peaks that are found below the threshold of $2\theta = 15^{o}$, which is the range in which clay minerals can be found when using Co-Kα radiation. From this point onward, peaks will be identified by the crystallographic spacing (d-spacing) in angstroms

(Å) which produces a peak at the given value of 2θ, as this is a more universal measure which is not dependent on the X-ray source used by the instrument.

The peaks of interest are: the chlorite peak at 14.3Å, which should be interpreted as hydroxy-interlayered vermiculite (HIV) within soil samples; the 2:1 clay mineral peak (the true mica and illite groups) at 10.1Å; and the 1:1 clay mineral (kaolin group) peak at 7.1Å (Chen, 1977). Peaks may not align exactly with these idealized values as natural materials do not conform to ideal models. The samples saturated with Mg^{2+} were most useful in demonstrating these peaks and these patterns and are used in all provided figures. Samples behaved similarly under the incremental heat treatments, so all samples are shown in the air-dried state for ease of comparison. All figures were labeled with d-spacings above the peaks of interest. Selected diffractograms, modified to emphasize features of interest, are provided as figures within this section. Additional diffractograms for the Mg^{2+}-saturated air-dried state for each sample are provided in Appendix A. No meaningful differences in the diffractogram patterns were observed in the test samples for R7-P2-B, R8-P1-C, R8-H1-C, and Q1-B relative to their respective controls. No data is available for Q1-R because it lacked sufficient clay fraction mass

.

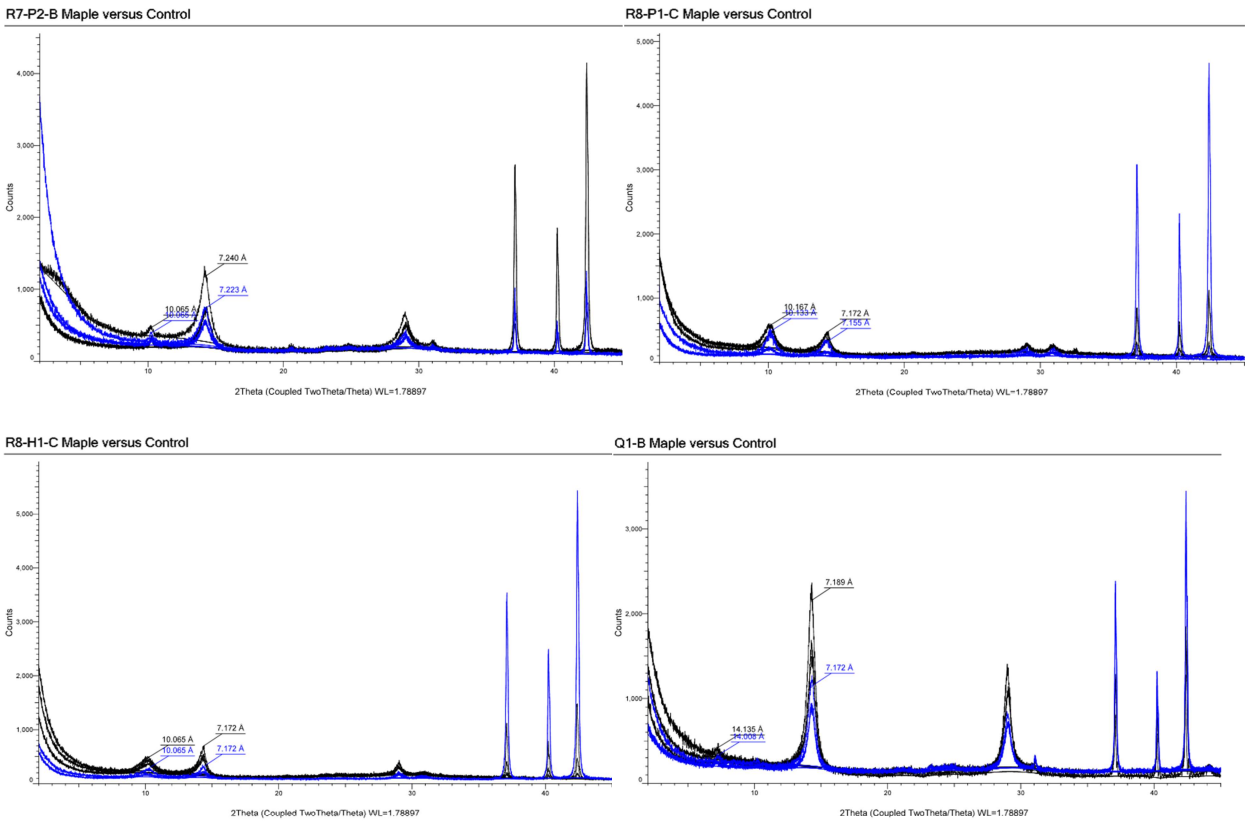

Figure 10. Miniatures of the diffractograms for R7-P2-B, R8-P1-C, R8-H1-C, and Q1-B (Mg-saturated, air-dried) in respective order from left to right and top to bottom. Controls are plotted in black and maples are plotted in blue. No meaningful changes to the XRD pattern are apparent for these samples. These diffractograms are reproduced at a larger scale in Appendix A.

Diffractograms of the air-dried slides for R1-C3-B experienced a decrease in the 14.3Å HIV peak intensity and an increase in the 10.1Å mica/illite peak intensity for the material in which maple seedlings had grown relative to the control material with no plants (Figure 11). In R1-C3-C, the mica/illite peak shifted (i.e., expanded) from 10.0Å to 10.3Å after the growth of the maples (Figure 12).

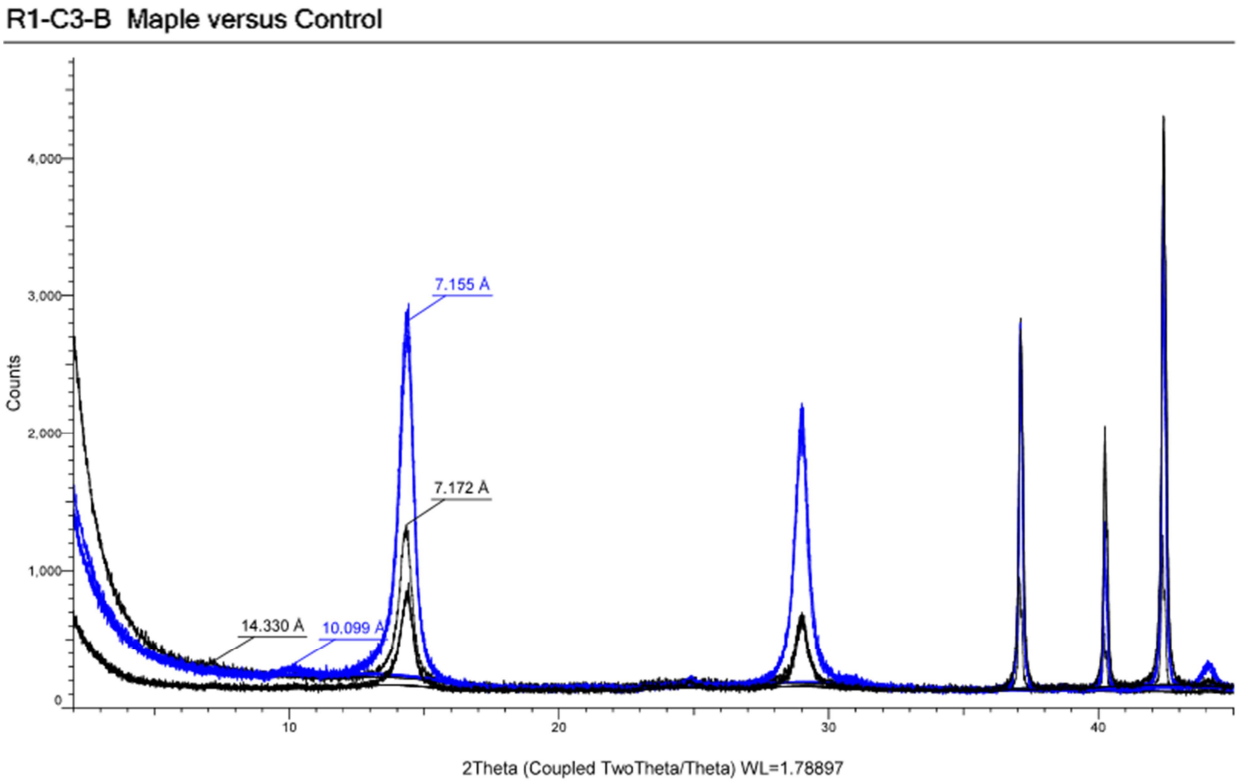

Figure 11. Diffractograms for R1-C3-B (Mg-saturated, air-dried) demonstrating reduced 14.3Å peak intensity and increased 10.1Å peak intensity for maples (blue) relative to controls (black).

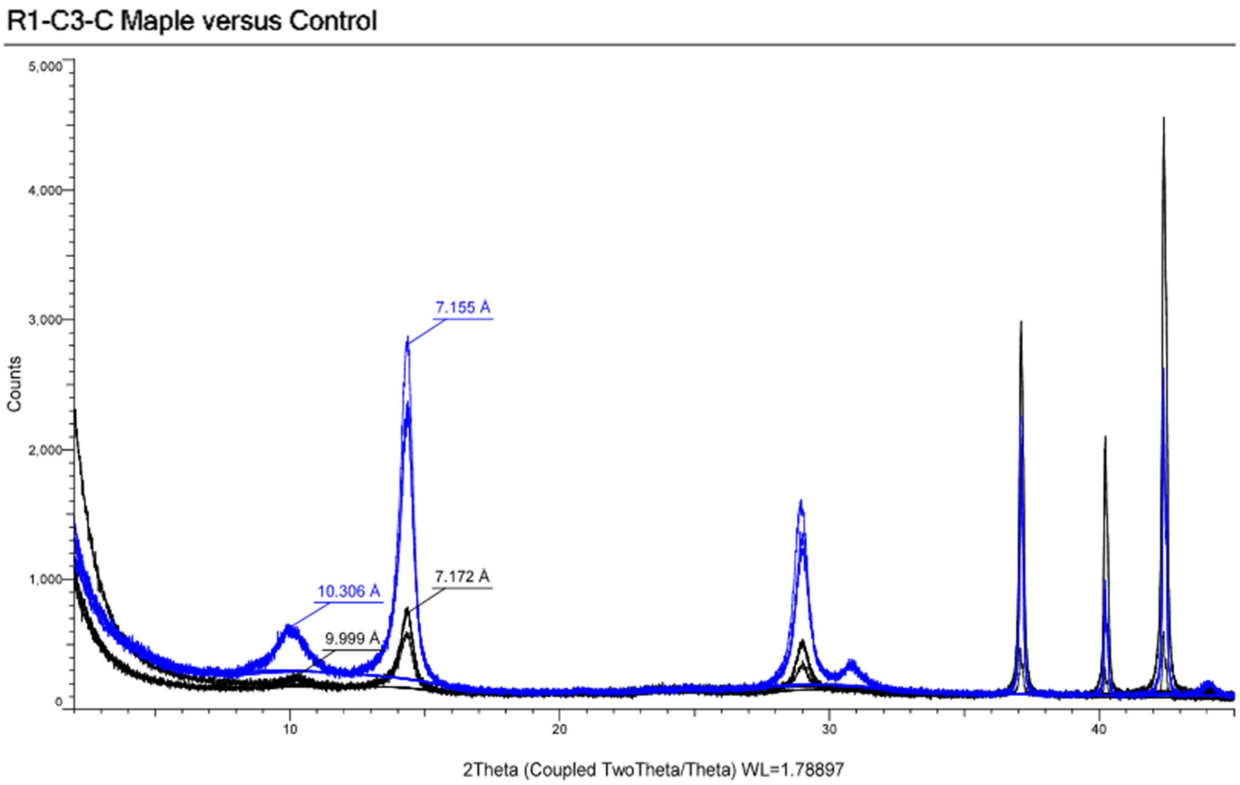

Figure 12. Diffractograms for R1-C3-C (Mg-saturated, air-dried) demonstrating shift in the mica/illite-like peak from 10.0Å in the controls (black) to 10.3Å after growth of maples (blue).

Diffractograms for Q1-C for both test materials and controls differ from the other samples due to the prominent presence of mixed-layer clay minerals. Mixed-layer clay minerals can be identified as an asymmetric peak or swath between the expected peaks for idealized clay minerals. One such swath appears very prominently from 10.0Å – 12.0Å. In the control, this mixed-layer phase produces a swath of equal X-ray intensity from 12.0Å down to 10.6Å before gradually tapering down in intensity by 10.0Å. After the growth of either plant species, this same behavior is present, but there is no reduction in X-ray intensity across the swath representing the mixed-layer phase all the way until its termination at 10.0Å (Figure 13.).

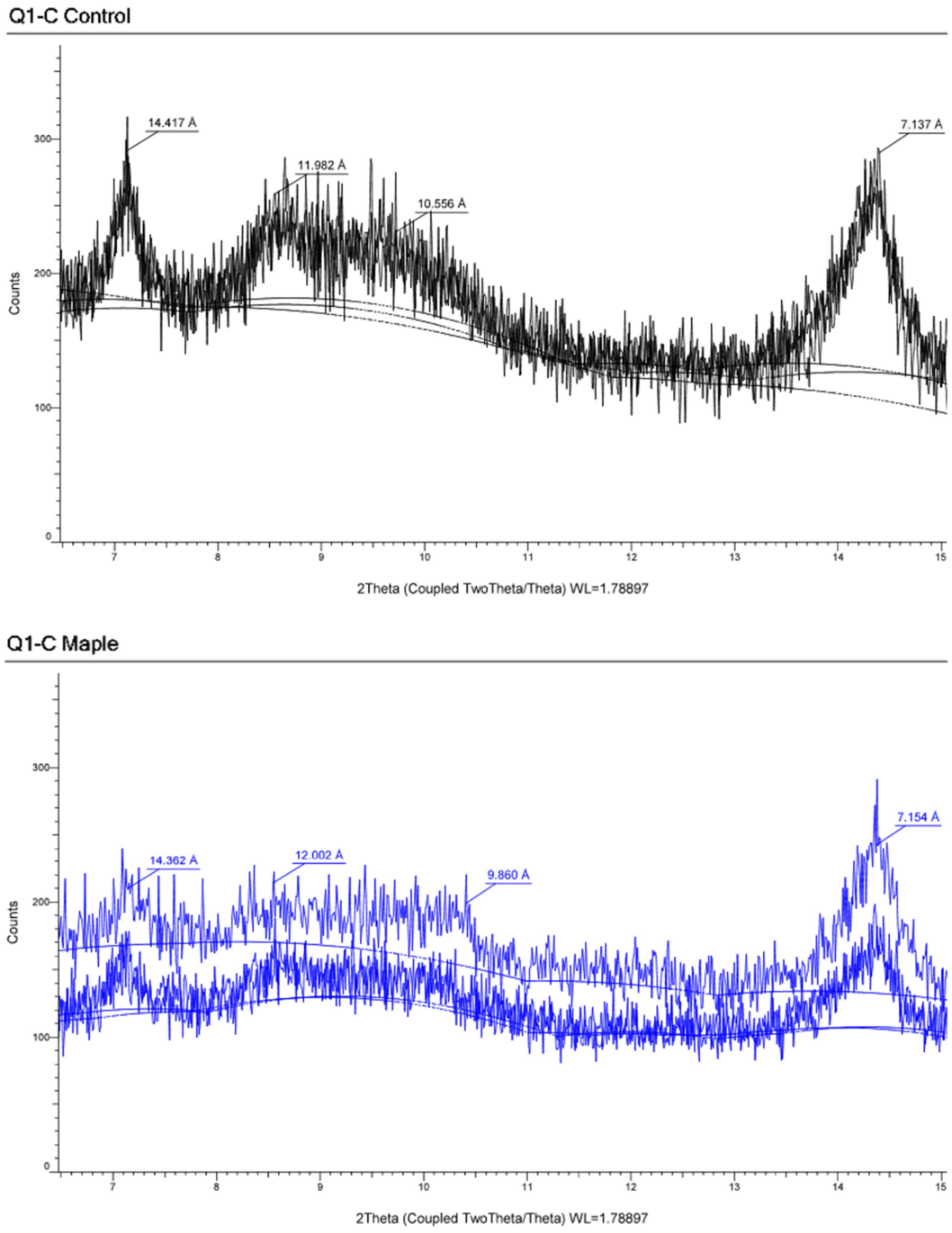

Figure 13. Diffractograms for Q1-C (Mg-saturated, air-dried), with emphasis placed on the behavior of the mixed-layer phase for the material in which maple seedlings had been grown. The plot has been enlarged to focus on the low-angle region in which the clay peaks are found. Pine samples behave similarly to maple samples; see Appendix A for all diffractograms.

The presence of mixed-layer clay minerals in materials used for R7-P2-C has been documented in prior research (Austin et al., 2020). The modelling done in this research demonstrated that the soil used for R7-P2-C has a clay fraction composed primarily of kaolinite (29-37 weight % depending on treatment) and several mixed-layer phases. The growth of maples imparts a broadening of the mica/illite peak which is much narrower and more defined in both the controls and the samples with pines. This comparatively defined peak is found at 10.0Å for controls and pines, which would correspond with the randomly ordered illite-biotite (IB50R0) and randomly ordered illite-vermiculite dominated by illite-like layers (IV(94-89)R0) identified by previous researchers (Austin et al., 2020). After the growth of maples, a broader peak can be found stretching from around 10.0Å – 10.3Å and gradually tapering off to either side (Figure 14.). This behavior is consistent with observed declines in EK noted above and implies that the growth of the maples is responsible for increasing the degree of disorder within this mineral phase (i.e., introducing more mixed-layer structures).

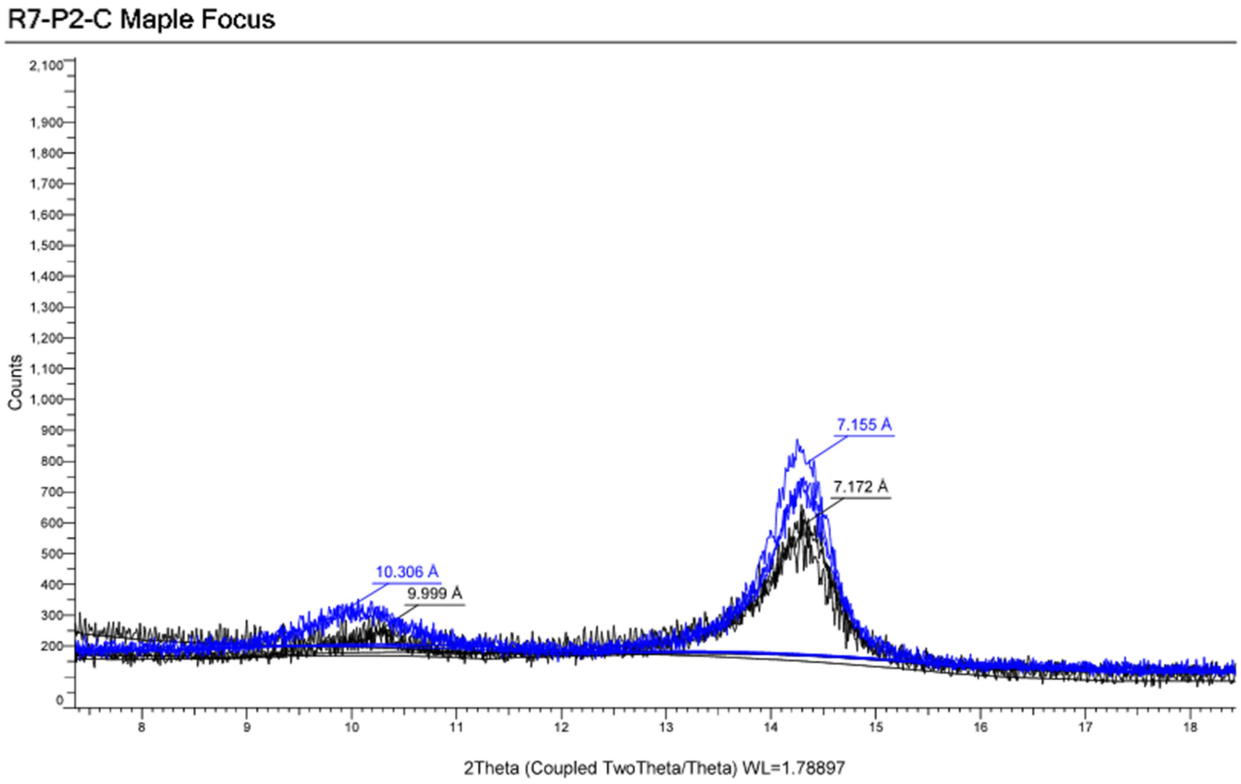

Figure 14. Diffractograms for R7-P2-C (Mg-saturated, air-dried) with emphasis on the shift from 10.0Å in controls (black) to 10.3Å after the growth of maples (blue).

In summary, not all diffractograms have demonstrable differences in the structural properties of the clay minerals following the growth of plants. In the case of pine growth, no alterations to clay mineral structure were observed at all outside of a very minor shifting in the high-intensity swath associated with a mixed-layer phase in Q1-C. In contrast, the behavior of increased mica/illite-like intensity was more prominent in the material subjected to maple growth for the same samples. Otherwise, all changes to clay mineral structure observed via XRD pattern analysis were found to occur after maple growth, not pine growth. These changes included an expansion of 0.3Å in the illite-like peak from 10.0Å to 10.3Å and increased structural disorder (i.e., broadened peaks).

4. DISCUSSION

Paired EK and XRD data indicate changes in mineral structure typically accompany substantial decreases in EK. Exceptions are R1-C3-B (where HIV was dominant over the mica/illite-like group clays, but no change was observed in EK) and R8-H1-C (in which EK was depleted, but no change were observed in the XRD pattern). In all other cases, this correlation holds true. In the case of R1-C3-C and R7-P2-C, EK decreased. In both of these substrates, the changes to the XRD pattern after the growth of maples included a shift of the mica/illite peak from 10.0Å to 10.3Å and broadening of peak.

In sample Q1-C, EK increased. For this sample, the changes to the XRD pattern after the growth of either maples or pines included an alteration of mixed-layer clay minerals that caused the mixed-layer swath to maintain an even intensity across its length rather than tapering off toward its lower d-spacing end. This was the only sample in which pines were observed to cause a change in clay mineral structure.

Based on these findings, chemical changes caused by maple growth may be manifesting in three main ways. The first of these is a loss of HIV (14Å) and a formation of illite-like clay (10Å), the peak shift observed in R1-C3-B. This change may be unrelated to potassium availability, given that no change in EK was observed in this sample. The second is observed in R1-C3-C and R7-P2-C. This change corresponds with the peak shift observed in these two samples and a depletion of EK reserves. The last possible change is a disordering of the mixed-layer peak (12-10Å) observed in Q1-C which is associated with an increase in EK reserves and structural changes to mixed layer clays if they are present.

Without knowing the mechanisms responsible for the shift from 10.0Å to 10.3Å and the disordering of the mixed-layer peak from 12-10Å, it is not possible to definitively relate these changes to the soil K cycle. Demonstrating their mechanism and linking it to the changes in EK would be a valuable avenue for further research.

Importantly, only Q1-C experienced noticeable changes to their XRD patterns as a consequence of pine growth, despite the maples and pines demonstrating the same behavior relative to EK consumption or production in most samples (except R7-P2-C and Q1-R). This observation implies fundamental differences between the nutrient uptake strategies employed by maples and the strategies employed by pines to extract potassium. Both trees and any associated mycorrhizal symbiotes achieve similar outcomes in terms of reducing potassium in the exchangeable pool (the depletions observed in R1-C3-C, R7-P2-C, and R8-H1-C), but the chemical mechanisms remain uncertain.

I hypothesized that pines (represented by *Pinus taeda*) and hardwoods (represented by *Acer rubrum*) would utilize different minerals as their primary sources of K^+ uptake, with hardwoods demonstrating a greater capacity to uptake K^+ from minerals found at great depth in the soil column, especially unmodified primary minerals (such as those present in Q1-R and to a lesser extent Q1-C). However, the XRD data suggest that regardless of mineral types, the chemical pathways employed by pines and maples (in conjunction with their respective mycorrhizal communities) are different chemical pathways that achieve similar effects. This is best demonstrated by HIV, illite-like, and mixed-layer peak shifts under maples that are not evident under pines. As such, I reject the initial hypothesis.

Based on my findings, I hypothesize for future research that *Acer rubrum* is more effective in its ability to restructure minerals for its nutrition than *Pinus taeda*. Testing this

hypothesis would require investigation into the chemical mechanisms responsible for the structural changes found in clay minerals during this study. These mechanisms would need to be identified and linked to nutrient uptake by the maples in order to confirm this hypothesis.

The findings of this study are overall in agreement with the work of previous researchers. For example, samples R8-P1-C and R8-H1-C are quite different chemically (considerably less EK in R8-P1-C than in R8-H1-C) despite coming from sites within the same research watershed and sharing a similar outward appearance in hand sample. Bulk chemical analysis of these samples performed in 2017 similarly demonstrated that the bulk K_2O weight % abundance was considerably lower in R8-P1 at the depth of sample R8-P1-C in this study (1.86 weight %) than in R8-H1 at the depth of sample R8-H1-C in this study (3.94 weight %). These samples also possess different trends in their rare earth element (REE) plots, implying different underlying parent material despite the relative geographic proximity (Austin and Schroeder, 2019). This interpretation is consistent with attempts to geologically map the region which posit the existence of variation in the underlying bedrock within the vicinity of watershed R8 (Jordan, 2020) that would account for these changes in initial bulk K_2O.

Bulk K_2O weight % based on the previous work of other researchers (Austin and Schroeder, 2019) for the materials associated with each of the R1-R8 samples used in this study are produced in Table 2 alongside the abundance of EK observed in the relevant control. The Q1 samples are novel to this study and had to be run separately. The opportunity for this analysis arose after the material had been mixed with 50% silica sand by volume in preparation for the growth experiment, so the provided values in Table 2 are corrected based on the assumption of an added 50.00 weight % SiO_2.

Sample	Bulk K_2O (Weight %)	Mean EK (ppm)
R1-C3-B	0.17	9.6 ± 5.0
R1-C3-C	0.76	18.5 ± 3.2
R7-P2-B	0.67	16.1 ± 3.2
R7-P2-C	0.84	17.4 ± 2.6
R8-P1-C	1.86	6.1 ± 0.9
R8-H1-C	3.94	14.0 ± 1.9
Q1-B	2.10†	30.5 ± 2.0
Q1-C	3.26†	16.7 ± 1.2
Q1-R	5.58†	6.0 ± 0.8

Table 2. Comparison of bulk K_2O as determined by previous workers (Austin and Schroeder, 2019) against observed EK in this study. Exchangeable potassium values are provided with 90% confidence intervals. The bulk K_2O data marked with a cross (†) are based on the material after the addition of 50% silica sand by volume. The raw data from analyzing these samples is presented in Appendix D, but is presented here after correcting for the added material on the assumption that the added silica sand represented 50.00 weight % SiO_2.

The comparisons in Table 2 demonstrate that the ratio of EK to bulk potassium is not equal across the CCZO, which is to be expected given the variety of hydrologic and biogeochemical conditions that could change this ratio. However, the ratios of EK to bulk potassium for one sample relative to the other one within the same excavation pit (R1-C3 samples and R7-P2 samples) or within the same research watershed (R8) remain roughly equal. The large increase in bulk K_2O at greater depth in R1-C3, the roughly unchanging bulk K_2O relative to depth in R7-P2, and the roughly doubled bulk K_2O in the hardwood plot relative to the pine plot for R8 are all mirrored by similar changes in the mean EK.

The exceptions to this trend are the quarry samples, which have progressively lower EK in the deeper horizons, regardless of the increases in bulk K_2O. This finding is still logical, as

the progressively deeper horizons represented by the quarry samples become more and more dominated by primary minerals which have abundant potassium in the form of micas and feldspars, but in structurally bound sites rather than accessible as EK.

Differences in overall bulk K_2O do correlate with whether observed changes in EK were decreases or increases. The CCZO samples had comparatively low bulk K_2O relative to the quarry samples, with the exception of R8-H1-C in which no change was noted. As noted previously, CCZO samples experienced a decrease in EK when changes were observed, whereas quarry samples experienced an increase in EK when changes were observed. Whether this correlation is a direct consequence of the differing bulk K_2O itself or rather a consequence of the mineral assemblages (primary minerals dominating in the quarry samples that experienced changes as opposed to secondary minerals dominating in the CCZO samples) is unclear.

Overall, the revised hypothesis that that *Acer rubrum* is more effective in its ability to restructure minerals for its nutrition than *Pinus taeda* builds upon the fundamentals of ecological succession. Ecologists have posited that nutrient cycles gradually change over the course of succession with an increasing prevalence of recycling and renewal in late-successional stage ecosystems as far back as some of the original works on old field succession (Odum, 1969). Recent work has built upon that foundation by demonstrating that regenerating pine forests lack the fine root density of less disturbed hardwood forests, which has been linked in part to the dominance of mid-successional pine species over late-successional hardwood species, with consequences for nutrient cycling (Hauser et al., 2020). Microbial (Billings et al., 2018) and mineralogical (Austin et al., 2018) consequences of the loss of deep rooting density further emphasize the potential importance of deep-rooted hardwoods to establishing fully developed nutrient cycles, particularly when accounting for the relevance of even primary minerals in

supplying K^+ to plants (Andrist-Rangel et al., 2006). This study further contributes to our understanding of the ways in which late-successional ecosystems with a greater diversity of tree species establish their biogeochemical cycles by approaching the differences between tree species through their interactions with K-bearing minerals.

5. SUMMARY

A greenhouse experiment was conducted for a 90-day growth period using both *Acer rubrum* and *Pinus taeda* raised in a selection of nine substrates from the Calhoun Critical Zone Observatory research area. Following the growth period, substrates were analyzed for exchangeable potassium (EK) concentration and XRD clay mineralogy. *A. rubrum* and *P. taeda* behaved similarly within substrates whether in raising or decreasing EK.

Regardless of these similarities in EK change, *P. taeda* had no effect on XRD clay mineral patterns outside of one exception (Q1-C). In contrast, *A. rubrum* altered clay minerals but changes differed depending on whether the maples increased or decreased the EK in a given substrate. These changes included peak shifts, structural alteration to mixed-layer clay minerals.

These findings suggest that *A. rubrum* and its associated mycorrhizae are more effective at restructuring clay minerals to satisfy nutritional demands than *P. taeda* and its mycorrhizae. Describing these mechanistic differences and linking them to the soil K cycle would improve our understanding of nutrient cycling dynamics for K^+ and the consequences of land use changes over time.

REFERENCES

Andrist-Rangel, Y., Hillier, S., Öborn, I., Lilly, A., Towers, W., Edwards, A. C., and Paterson, E., 2010, Assessing potassium reserves in northern temperate grassland soils: A perspective based on quantitative mineralogical analysis and aqua-regia extractable potassium: Geoderma, v. 158, no. 3-4, p. 303-314.

Andrist-Rangel, Y., Simonsson, M., Andersson, S., Öborn, I., and Hillier, S., 2006, Mineralogical budgeting of potassium in soil: A basis for understanding standard measures of reserve potassium: Journal of Plant Nutrition and Soil Science, v. 169, no. 5, p. 605-615.

April, R., and Keller, D., 1990, Mineralogy of the Rhizosphere in Forest Soils of the Eastern United States: Mineralogic Studies of the Rhizosphere: Biogeochemistry, v. 9, no. 1, p. 1-18.

Austin, J. C., Richter, D. D., and Schroeder, P. A., 2020, Quantification of Mixed-Layer Clays in Multiple Saturation States Using NEWMOD2: Implications for the Potassium Uplift Hypothesis in the SE United States: Clays and Clay Minerals, v. 68, no. 1, p. 67-80.

Austin, J. C., and Schroeder, P. A., 2019, CCZO -- Soil Geochemistry -- Calhoun CZO -- (2016-2016): Hydroshare.

Austin, J. J. C., Perry, A. A., Richter, D. D. D., and Schroeder, P. P. A., 2018, Modifications of 2:1 clay minerals in a kaolinite-dominated Ultisol under changing land-use regimes: Clays and Clay Minerals.

Banwart, S., Menon, M., Bernasconi, S. M., Bloem, J., Blum, W. E. H., Souza, D. M. d., Davidsdotir, B., Duffy, C., Lair, G. J., Kram, P., Lamacova, A., Lundin, L., Nikolaidis, N. P., Novak, M., Panagos, P., Ragnarsdottir, K. V., Reynolds, B., Robinson, D., Rousseva, S., de Ruiter, P., van Gaans, P., Weng, L., White, T., and Zhang, B., 2012, Soil processes and functions across an international network of Critical Zone Observatories: Introduction to experimental methods and initial results: Comptes Rendus Geoscience, v. 344, no. 11-12, p. 758-772.

Barré, P., Montagnier, C., Chenu, C., Abbadie, L., and Velde, B., 2007a, Clay minerals as a soil potassium reservoir: observation and quantification through X-ray diffraction: Plant and Soil, v. 302, no. 1-2, p. 213-220.

Barré, P., Velde, B., Catel, N., and Abbadie, L., 2007b, Soil-plant potassium transfer: impact of plant activity on clay minerals as seen from X-ray diffraction: Plant and Soil, v. 292, no. 1-2, p. 137-146.

Billings, S. A., Hirmas, D., Sullivan, P. L., Lehmeier, C. A., Bagchi, S., Min, K., Brecheisen, Z., Hauser, E., Stair, R., Flournoy, R., and Richter, D. D. D., 2018, Loss of deep roots limits biogenic agents of soil development that are only partially restored by decades of forest regeneration: Elementa Science of the Anthropocene, v. 6, no. 1.

Bonneville, S., Bray, A. W., and Benning, L. G., 2016, Structural Fe(II) Oxidation in Biotite by an Ectomycorrhizal Fungi Drives Mechanical Forcing: Environ Sci Technol, v. 50, no. 11, p. 5589-5596.

Cama, J., and Ganor, J., 2006, The effects of organic acids on the dissolution of silicate minerals: A case study of oxalate catalysis of kaolinite dissolution: Geochimica et Cosmochimica Acta, v. 70, no. 9, p. 2191-2209.

Chen, P.-Y., 1977, Table of key lines in X-ray powder diffraction of minerals in clays and associated rocks Indiana Geological Survey Occasional Paper, v. 21.

Coughlan, M., Nelson, D., Lonneman, M., and Block, A., 2017, Historical Land Use Dynamics in the Highly Degraded Landscape of the Calhoun Critical Zone Observatory: Land, v. 6, no. 2.

Evans, H. J., and Sorger, G. J., 1966, Role of mineral elements with emphasis on the univalent cations: Annual Review of Plant Physiology, v. 17, p. 47-76.

Fox, T. R., and Comerford, N. B., 1990, Low-Molecular-Weight Organic Acids in Selected Forest Soils of the Southeastern USA: Soil Science Society of America Journal, v. 9, p. 25-32.

Hauser, E., Richter, D. D., Markewitz, D., Brecheisen, Z., and Billings, S. A., 2020, Persistent anthropogenic legacies structure depth dependence of regenerating rooting systems and their functions: Biogeochemistry, v. 147, p. 259-275.

Jobbágy, E. G., and Jackson, R. B., 2004, The Uplift of Soil Nutrients by Plants: Biogeochemical Consequences across Scales: Ecology, v. 85, no. 9, p. 2380-2389.

Jordan, B., 2020, Geology of the Calhoun Critical Zone Observatory [M.S., Geology Masters of Science]: University of Georgia.

Lian, B., Wang, B., Pan, M., Liu, C., and Teng, H. H., 2008, Microbial release of potassium from K-bearing minerals by thermophilic fungus Aspergillus fumigatus: Geochimica et Cosmochimica Acta, v. 72, no. 1, p. 87-98.

Lundström, U. S., and Öhman, L.-O., 1990, Dissolution of feldspars in the presence of natural, organic solutes: Journal of Soil Science, v. 41, p. 359-369.

Lybrand, R. A., Austin, J. C., Fedenko, J., Gallery, R. E., Rooney, E., Schroeder, P. A., Zaharescu, D. G., and Qafoku, O., 2019, A coupled microscopy approach to assess the nano-landscape of weathering: Sci Rep, v. 9, no. 1, p. 5377.

Markewitz, D., and Richter, D. D. D., 2000, Long-term soil potassium availability from a Kanhapludult to an aggrading loblolly pine ecosystem: Forest Ecology and Management, v. 130, p. 109-129.

McMaster, T. J., 2012, Atomic Force Microscopy of the fungi-mineral interface: applications in mineral dissolution, weathering and biogeochemistry: Curr Opin Biotechnol, v. 23, no. 4, p. 562-569.

Mobley, M., Lajtha, K., Kramer, M. G., Bacon, A. R., Heine, P. R., and Richter, D. D., 2015, Surficial gains and subsoil losses of soil carbon and nitrogen during secondary forest development: Global Change Biology, v. 21, no. 2, p. 986-996.

Odum, E. P., 1969, The Strategy of Ecosystem Development: Science, v. 164, no. 3877, p. 262-270.

Page, A. L., 1982, Methods of Soil Analysis: Part 2. Chemical and Microbiological Properties: Madison, WI, American Society of Agronomy, Soil Science Society of America.

Richter, D. D., and Markewitz, D., 1995, How Deep Is Soil?: BioScience, v. 45, no. 9, p. 600-609.

Rosenstock, N. P., Berner, C., Smits, M. M., Kram, P., and Wallander, H., 2016, The role of phosphorus, magnesium and potassium availability in soil fungal exploration of mineral nutrient sources in Norway spruce forests: New Phytol, v. 211, no. 2, p. 542-553.

Rosling, A., Lindahl, B. D., and Finlay, R. D., 2004, Carbon allocation to ectomycorrhizal roots and mycelium colonising different mineral substrates: New Phytologist, v. 162, no. 3, p. 795-802.

Schroeder, P. A., 2018, Clays in the Critical Zone, Cambridge, UK, Cambridge University Press.

Shakeri, S., and Abtahi, S. A., 2018, Potassium forms in calcareous soils as affected by clay minerals and soil development in Kohgiluyeh and Boyer-Ahmad Province, Southwest Iran: Journal of Arid Land, v. 10, no. 2, p. 217-232.

Trimble, S. W., 2008, Man-induced soil erosion on the southern Piedmont,1700–1970, Department of Geography, UCLA, Los Angeles, California, USA, Soil and Water Conservation Society.

van Hees, P. A. W., Rosling, A., Lundström, U. S., and Finlay, R. D., 2006, The biogeochemical impact of ectomycorrhizal conifers on major soil elements (Al, Fe, K and Si): Geoderma, v. 136, no. 1-2, p. 364-377.

Vinichuk, M., Taylor, A. F., Rosen, K., and Johanson, K. J., 2010, Accumulation of potassium, rubidium and caesium (133Cs and 137Cs in various fractions of soil and fungi in a Swedish forest: Sci Total Environ, v. 408, no. 12, p. 2543-2548.

Wallander, H., and Wickman, T., 1999, Biotite and microcline as potassium sources in ectomycorrhizal and non-mycorrhizal Pinus sylvestris seedlings: Mycorrhiza, v. 9, p. 25-32.

Woehrel, M. L., and Light, W. H., 2017, Mushrooms of the Georgia Piedmont & Southern Appalachians, Athens, GA, University of Georgia Press, 647 p.:

Xiao, B., Lian, B., Sun, L., and Shao, W., 2012, Gene transcription response to weathering of K-bearing minerals by Aspergillus fumigatus: Chemical Geology, v. 306-307, p. 1-9.

Yuan, L., Huang, J., Li, X., and Christie, P., 2004, Biological mobilization of potassium from clay minerals by ectomycorrhizal fungi and eucalypt seedling roots: Plant and Soil, v. 262, p. 351-361.

APPENDIX A

Full-page reproductions of the Mg-saturated, air-dried sample diffractograms for each sample are provided in this section. Samples with seedlings are plotted in blue (maples) or green (pines) against the controls (in black).

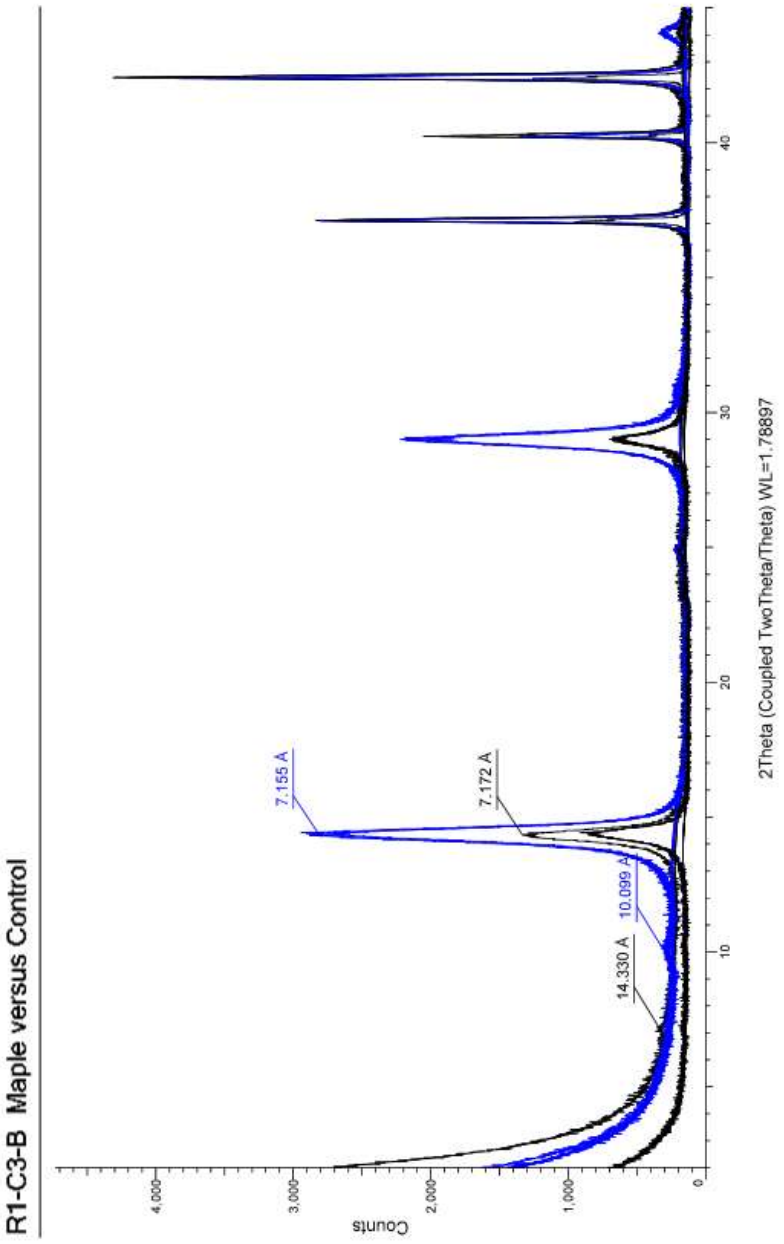
R1-C3-B Maple versus Control
Counts
4,000
3,000
2,000
1,000
0
10
20
30
40
7.155 A
7.172 A
10.099 A
14.330 A
2Theta (Coupled TwoTheta/Theta) WL=1.78897

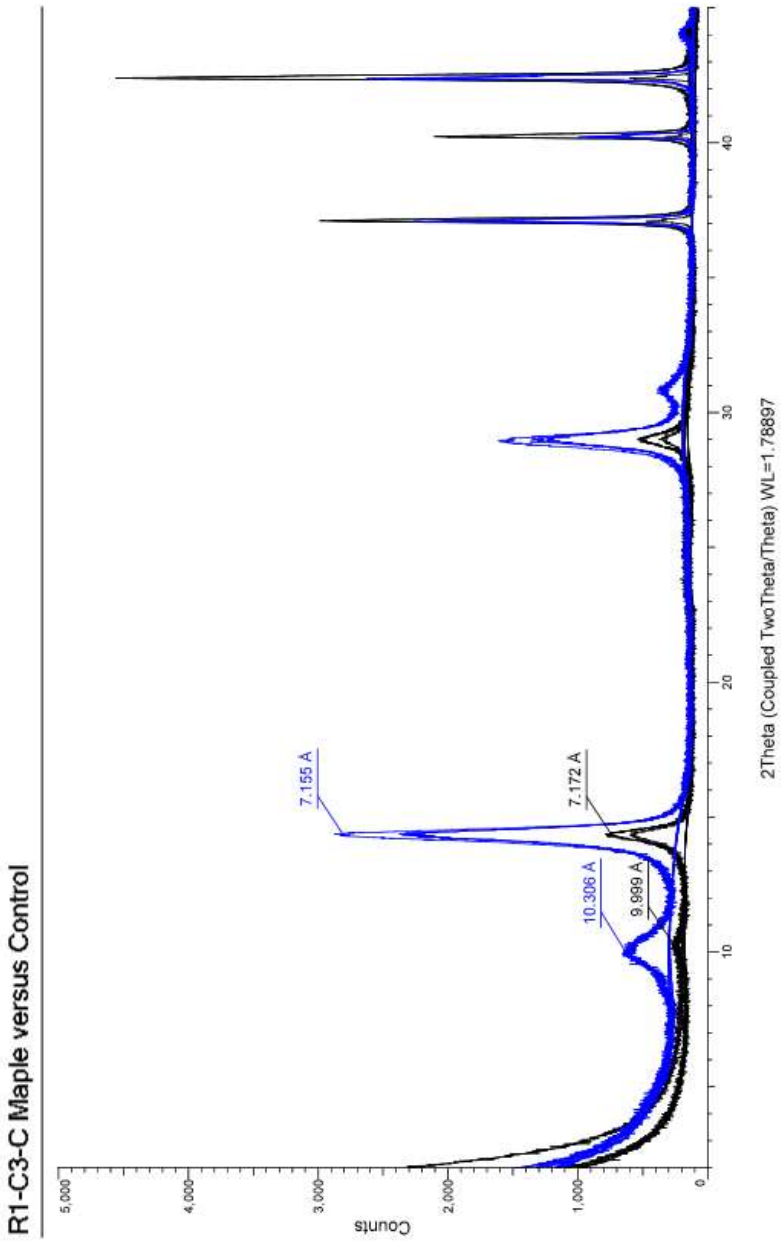
R1-C3-C Maple versus Control
Counts
5,000
4,000
3,000
2,000
1,000
0
10
20
30
40
7.155 Å
7.172 Å
10.306 Å
9.999 Å
2Theta (Coupled TwoTheta/Theta) WL=1.78897

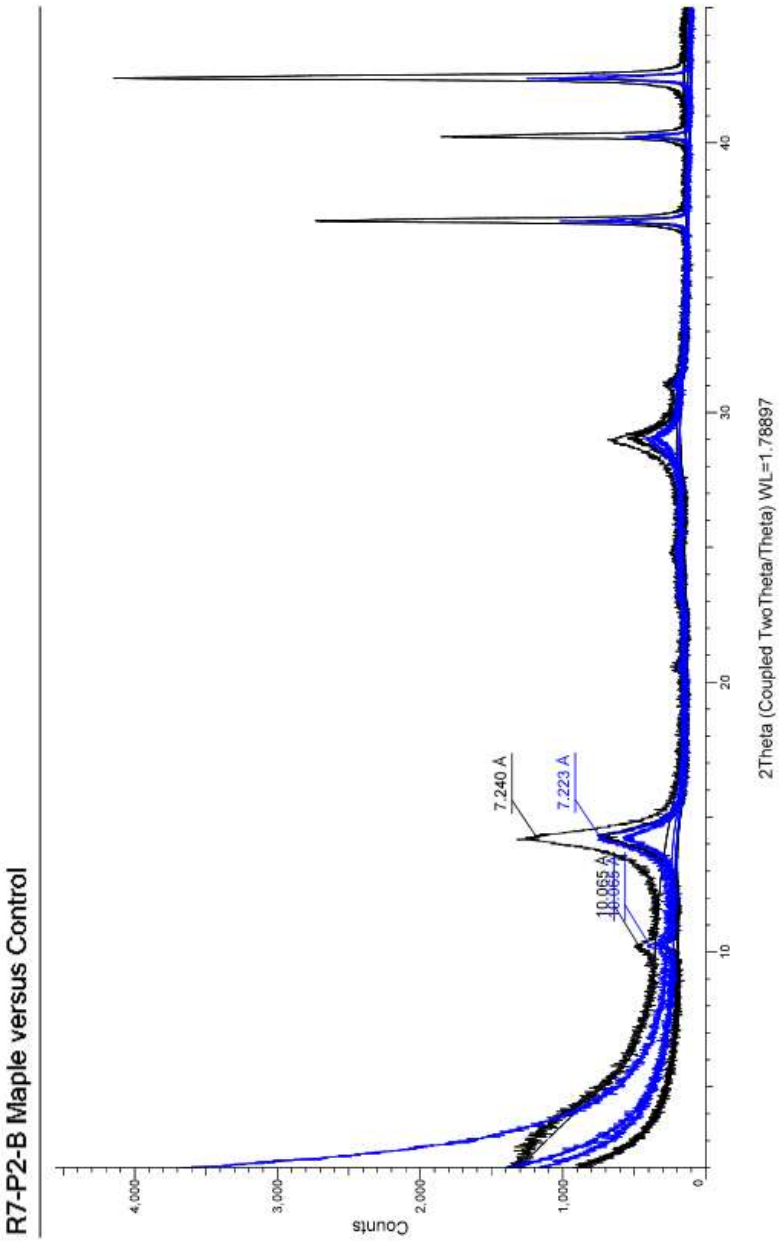
R7-P2-B Maple versus Control
Counts
4,000
3,000
2,000
1,000
0
10
20
30
40
7.240 A
7.223 A
10.065 A
2Theta (Coupled TwoTheta/Theta) WL=1.78897

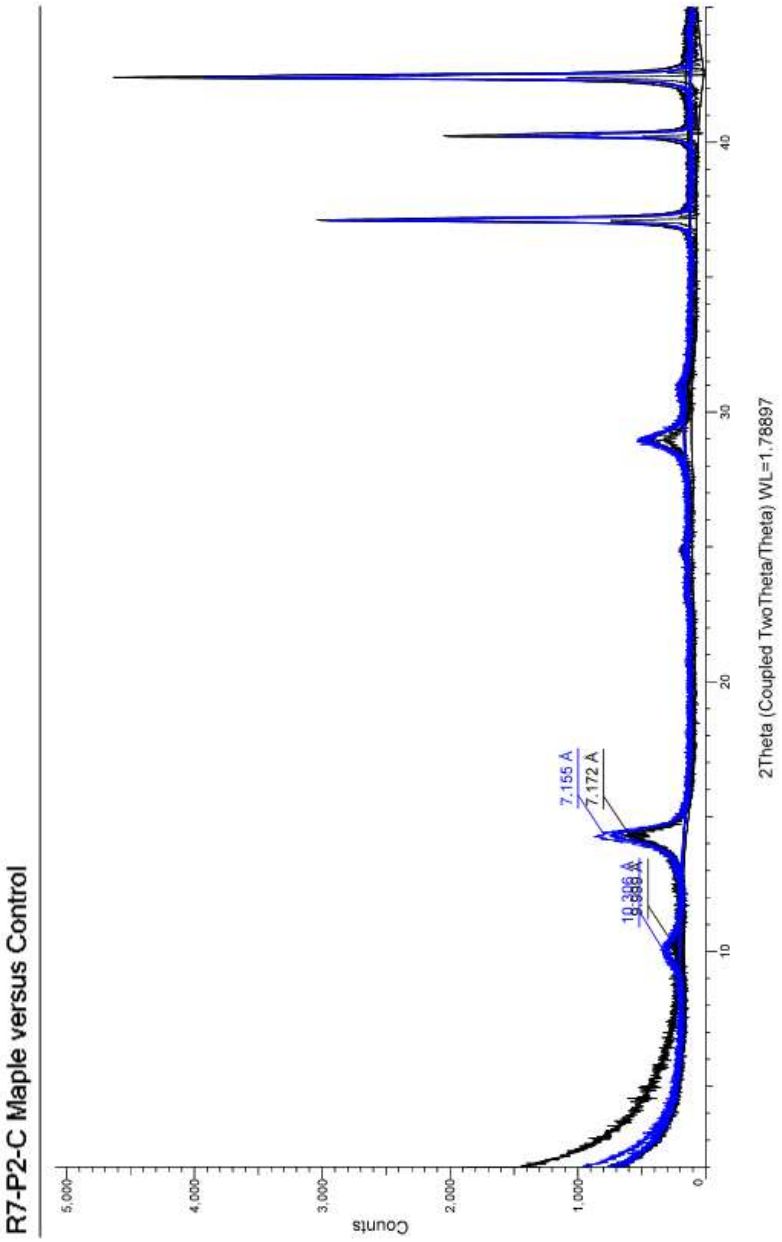
R7-P2-C Maple versus Control
Counts
5,000
4,000
3,000
2,000
1,000
0
10
20
30
40
7.155 A
7.172 A
2Theta (Coupled TwoTheta/Theta) WL=1.78897

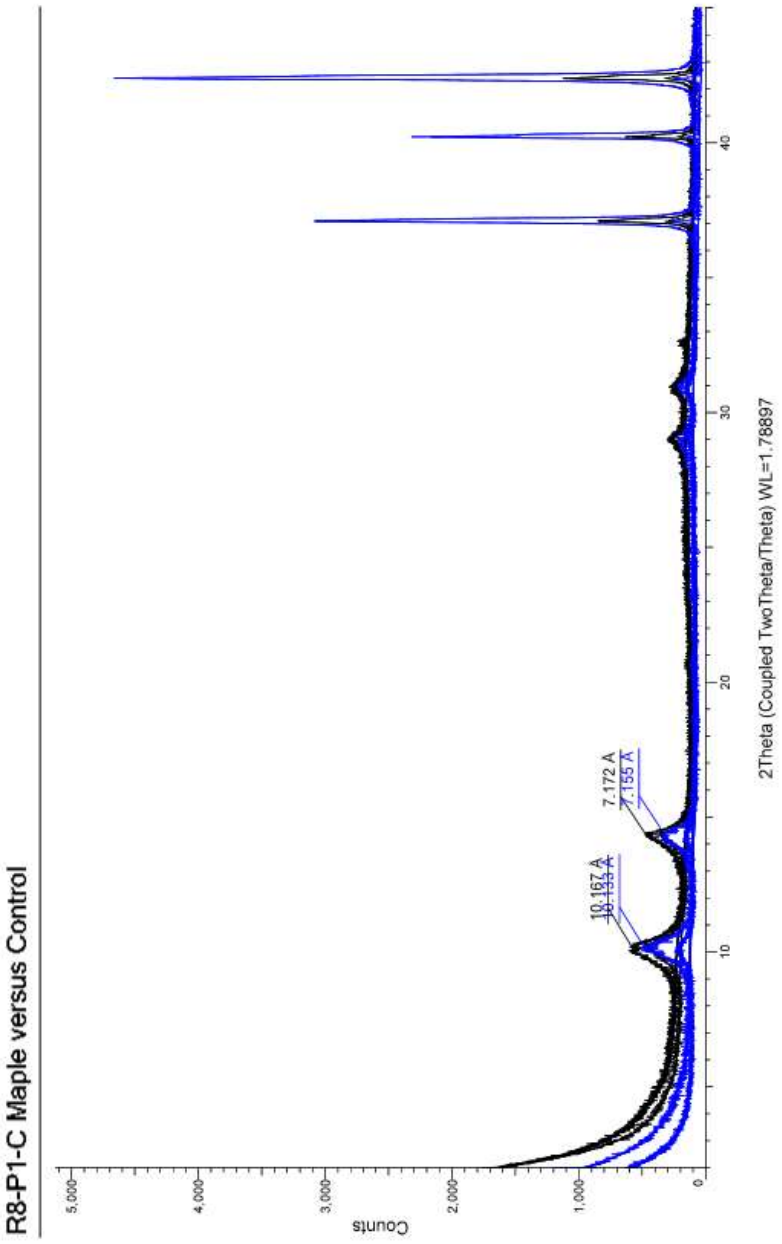
R8-P1-C Maple versus Control
Counts
5,000
4,000
3,000
2,000
1,000
0
10.167 A
10.133 A
7.172 A
7.155 A
10
20
30
40
2Theta (Coupled TwoTheta/Theta) WL=1.78897

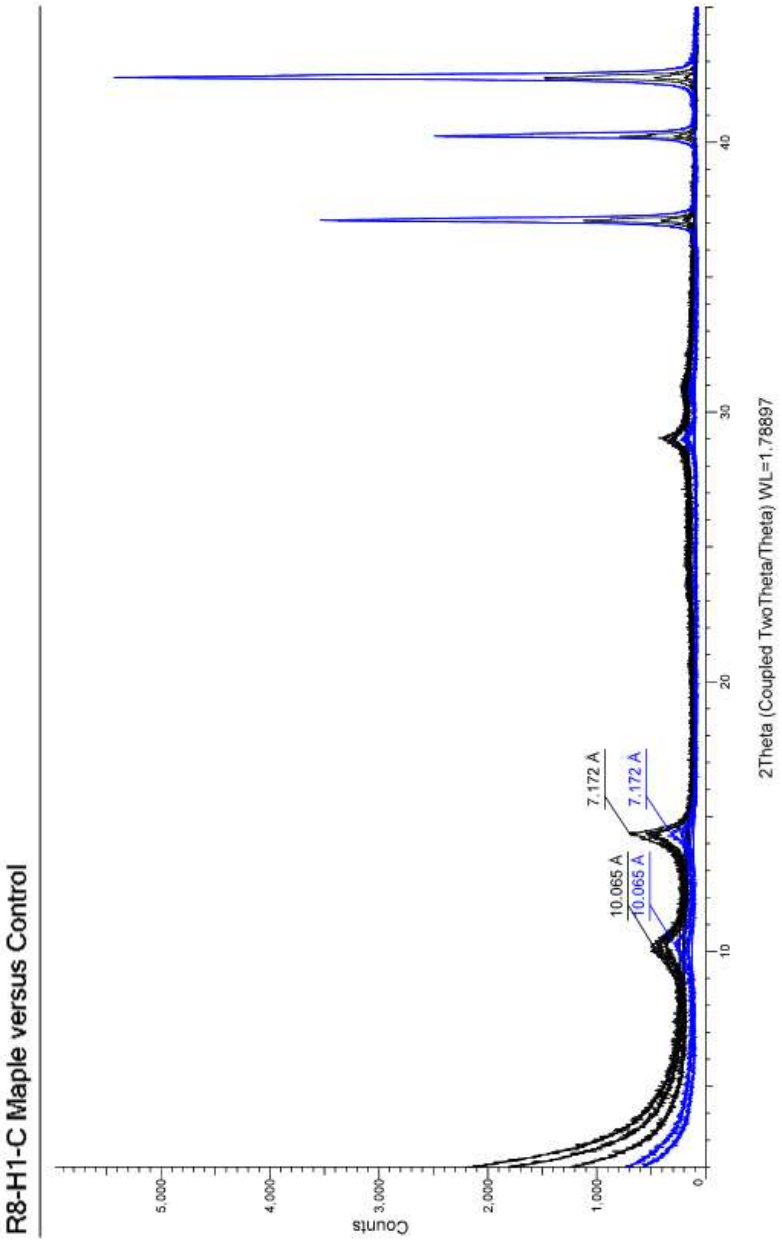
R8-H1-C Maple versus Control
Counts
5,000
4,000
3,000
2,000
1,000
0
10
20
30
40
2Theta (Coupled TwoTheta/Theta) WL=1.78897
7.172 Å
7.172 Å
10.065 Å
10.065 Å

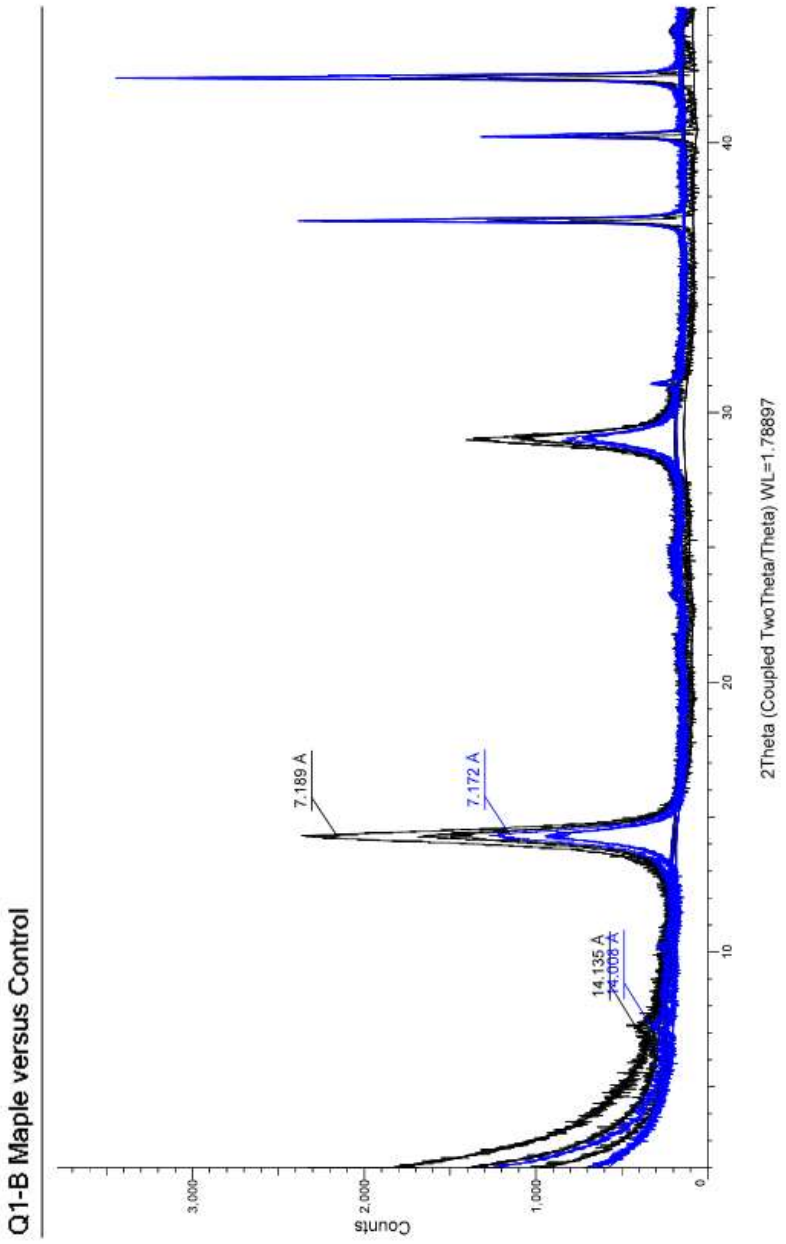
Q1-B Maple versus Control
Counts
3,000
2,000
1,000
0
7.189 Å
7.172 Å
14.135 Å
14.008 Å
10
20
30
40
2Theta (Coupled TwoTheta/Theta) WL=1.78897

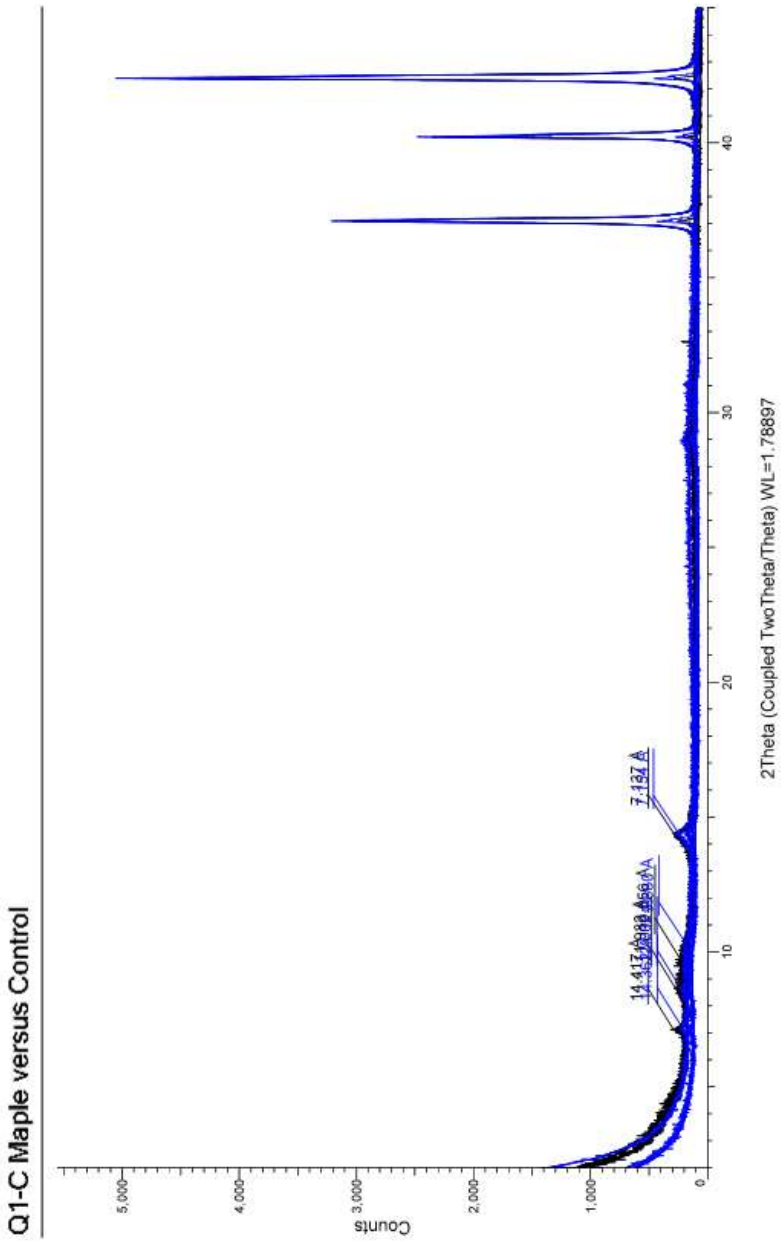
Q1-C Maple versus Control
Counts
5,000
4,000
3,000
2,000
1,000
0
10
20
30
40
7.137 Å
2Theta (Coupled TwoTheta/Theta) WL=1.78897

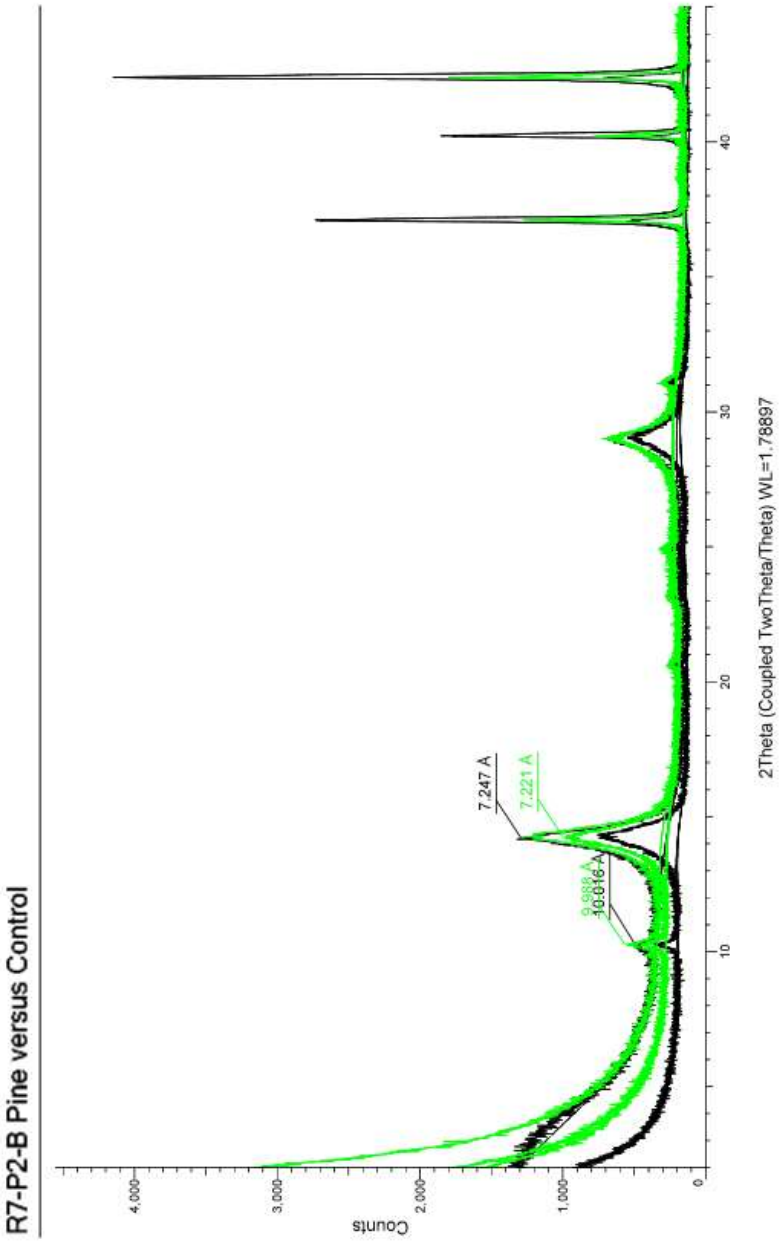
R7-P2-B Pine versus Control
Counts
4.000
3.000
2.000
1.000
0
10
20
30
40
7.247 A
7.221 A
9.698 A
10.016 A
2Theta (Coupled TwoTheta/Theta) WL=1.78897

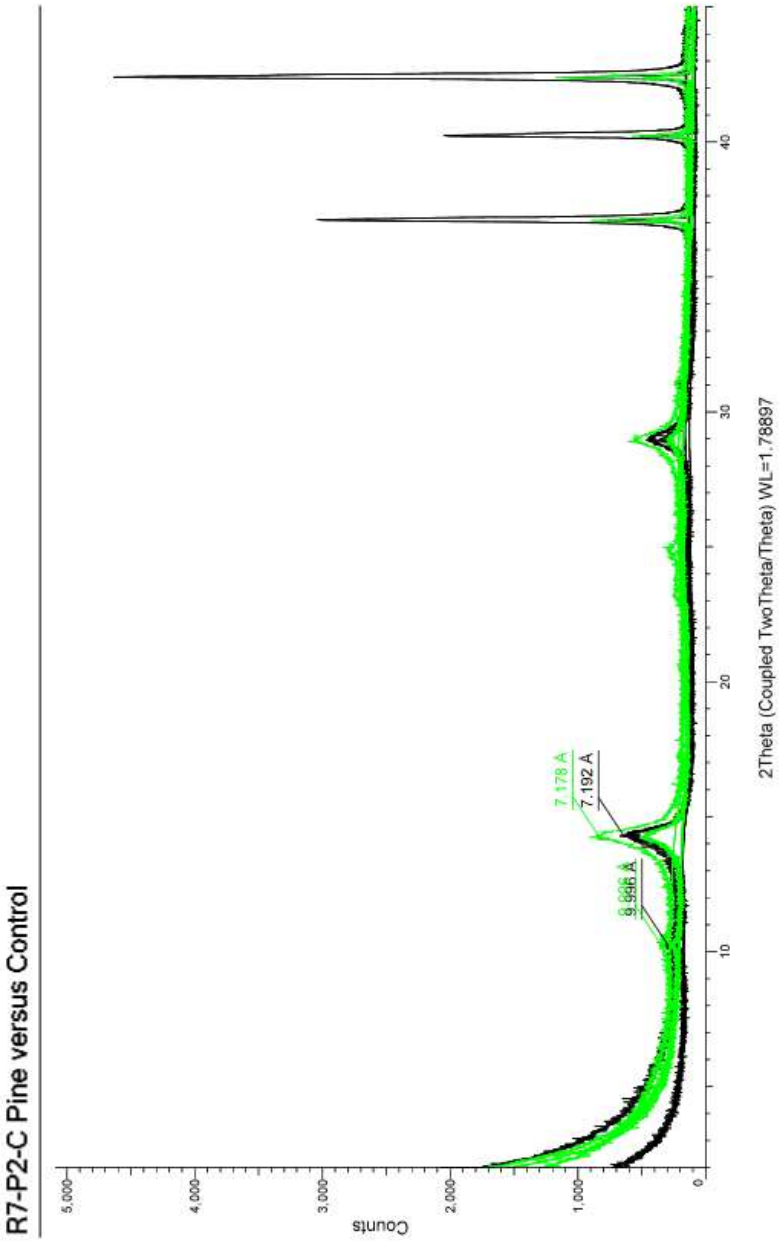
R7-P2-C Pine versus Control
Counts
5.000
4.000
3.000
2.000
1.000
0
10
20
30
40
7.178 A
7.192 A
9.996 A
2Theta (Coupled TwoTheta/Theta) WL=1.78897

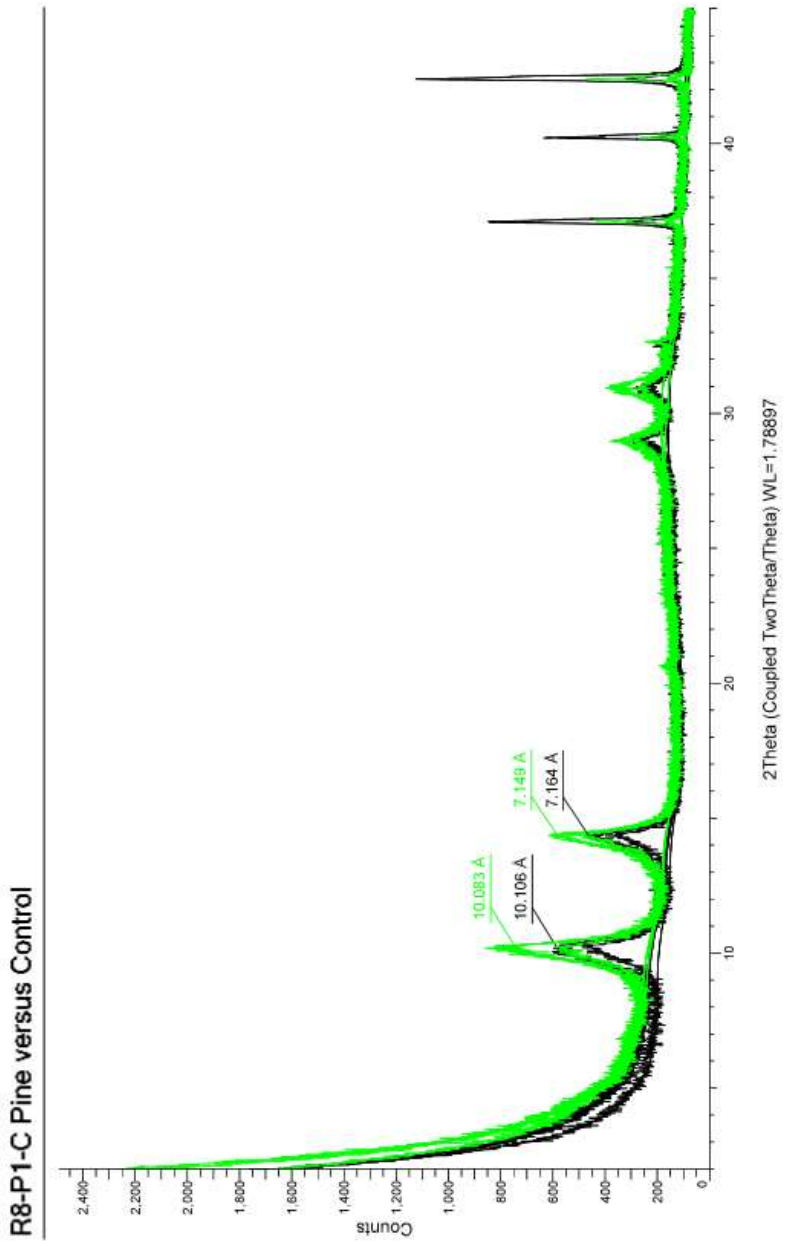
R8-P1-C Pine versus Control
Counts
2,400
2,200
2,000
1,800
1,600
1,400
1,200
1,000
800
600
400
200
0
10
20
30
40
10.083 A
10.106 A
7.149 A
7.164 A
2Theta (Coupled TwoTheta/Theta) WL=1.78897

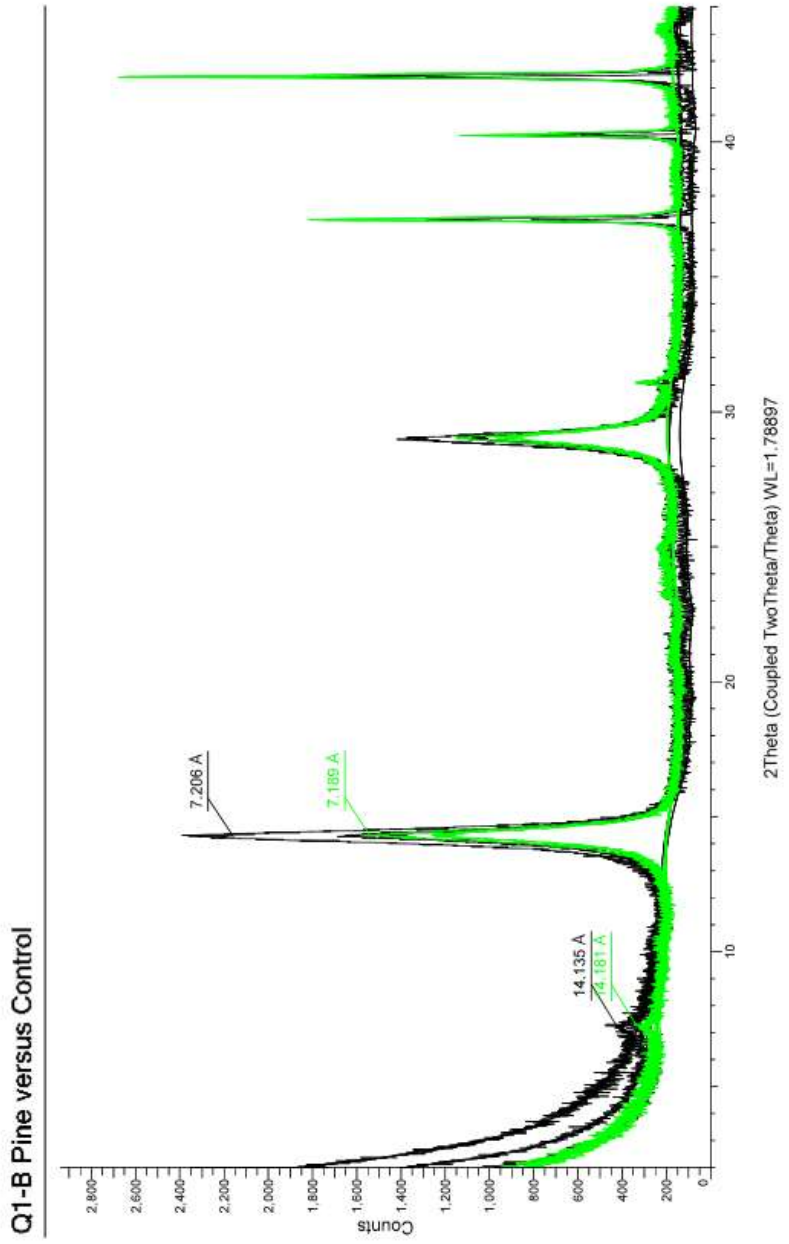
Q1-B Pine versus Control
Counts
2Theta (Coupled TwoTheta/Theta) WL=1.78897
7.206 A
7.189 A
14.135 A
14.181 A

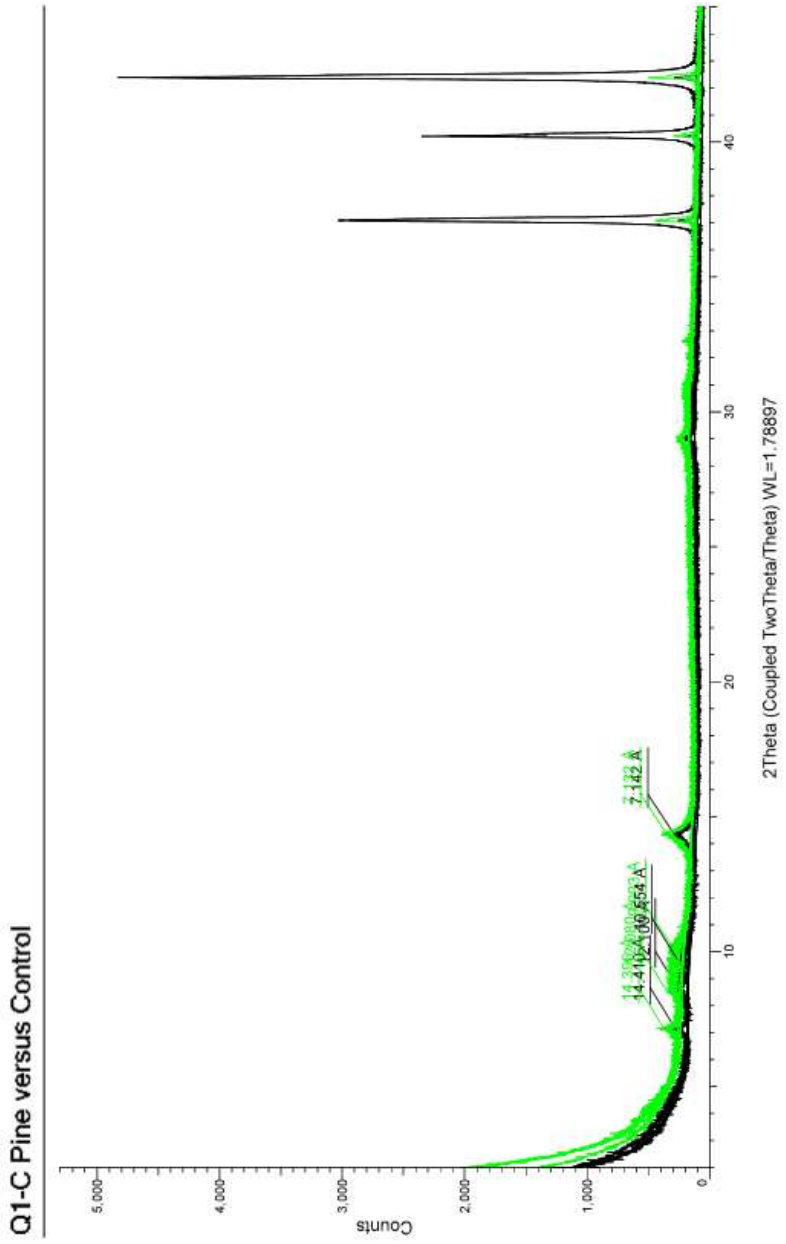
Q1-C Pine versus Control
Counts
5.000
4.000
3.000
2.000
1.000
0
10
20
30
40
7.142 Å
14.410 Å
2Theta (Coupled TwoTheta/Theta) WL=1.78897

APPENDIX B: RESEARCH TIMELINE

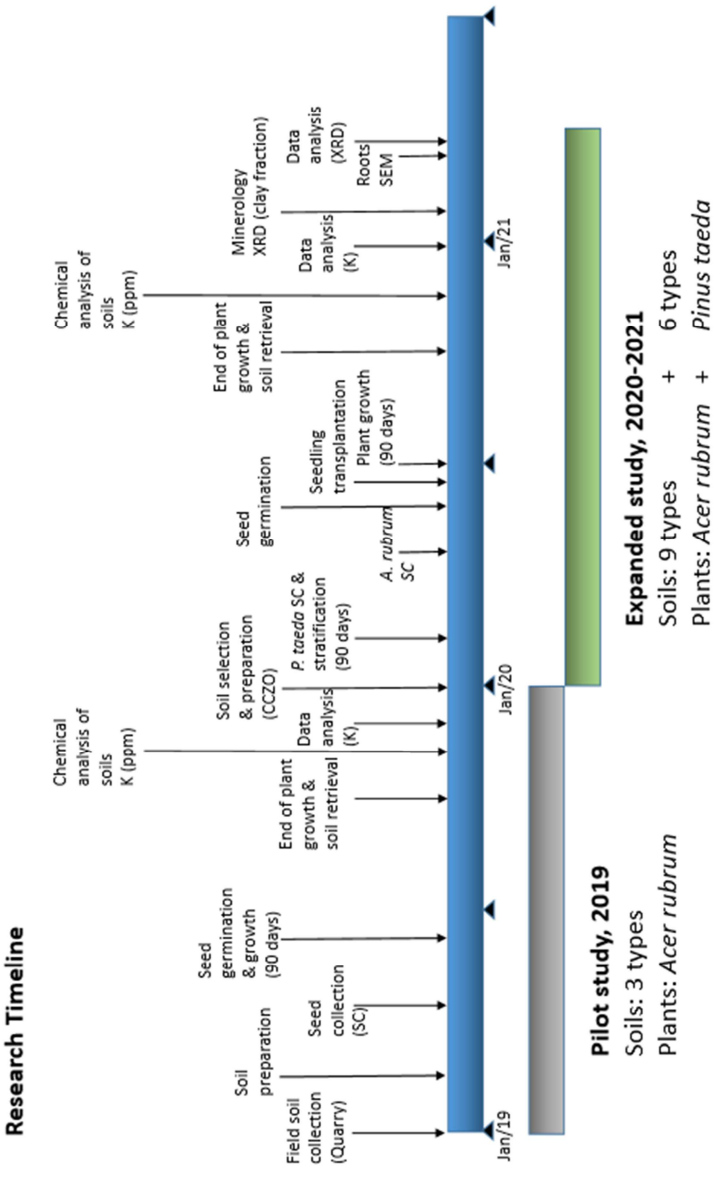

APPENDIX C: SEM IMAGERY

R1-C3-B, Maple root fiber

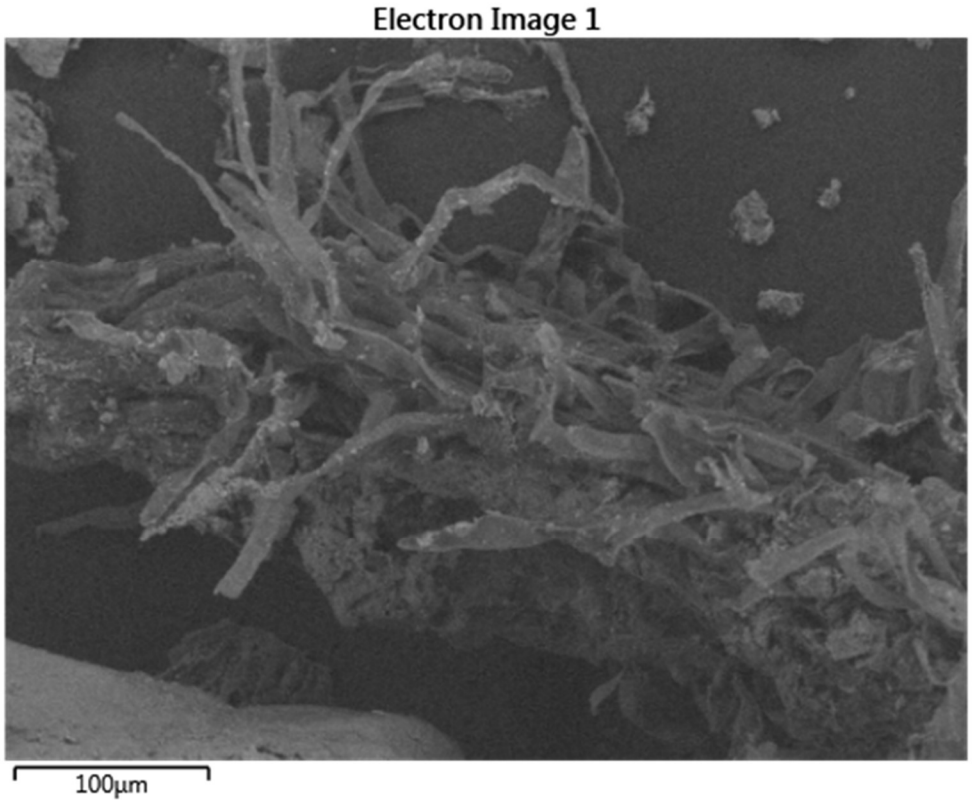

R1-C3-C, Maple root fiber

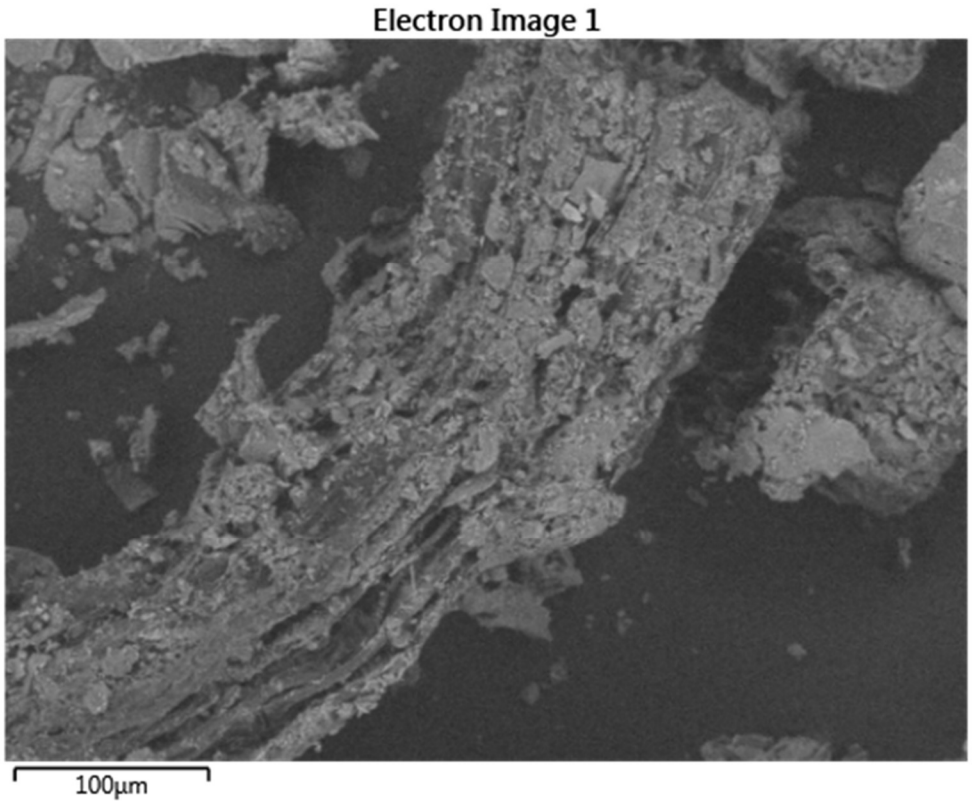

R7-P2-B, Maple root fiber

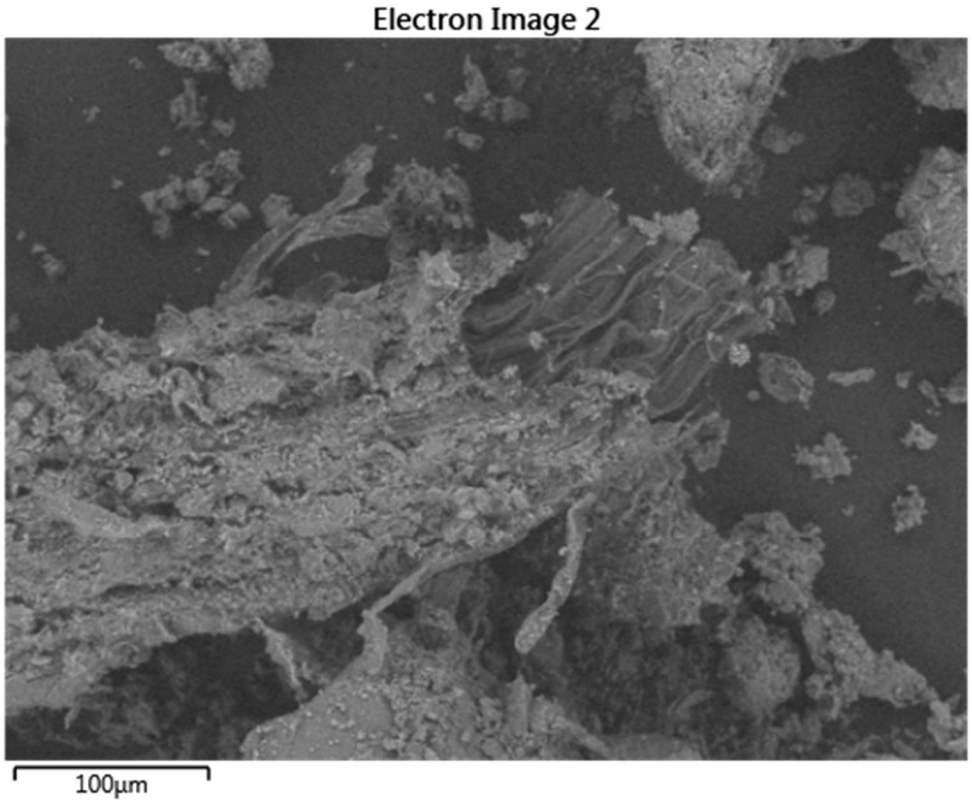

R7-P2-B, Pine root fiber

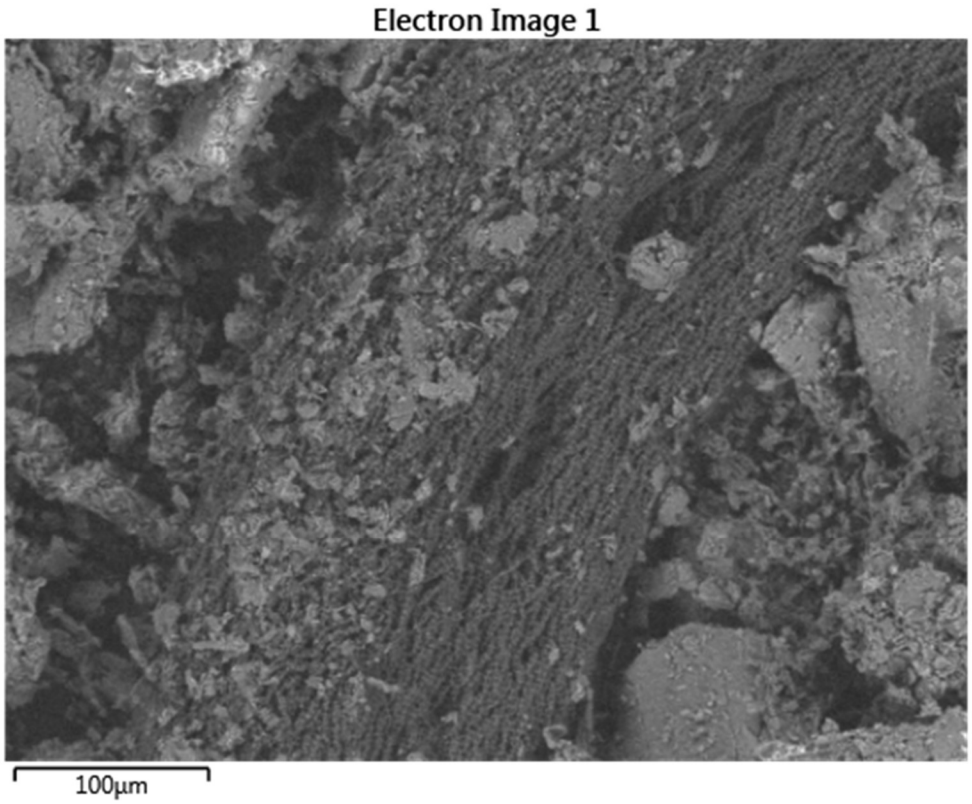

R8-H1-C, Maple root fiber

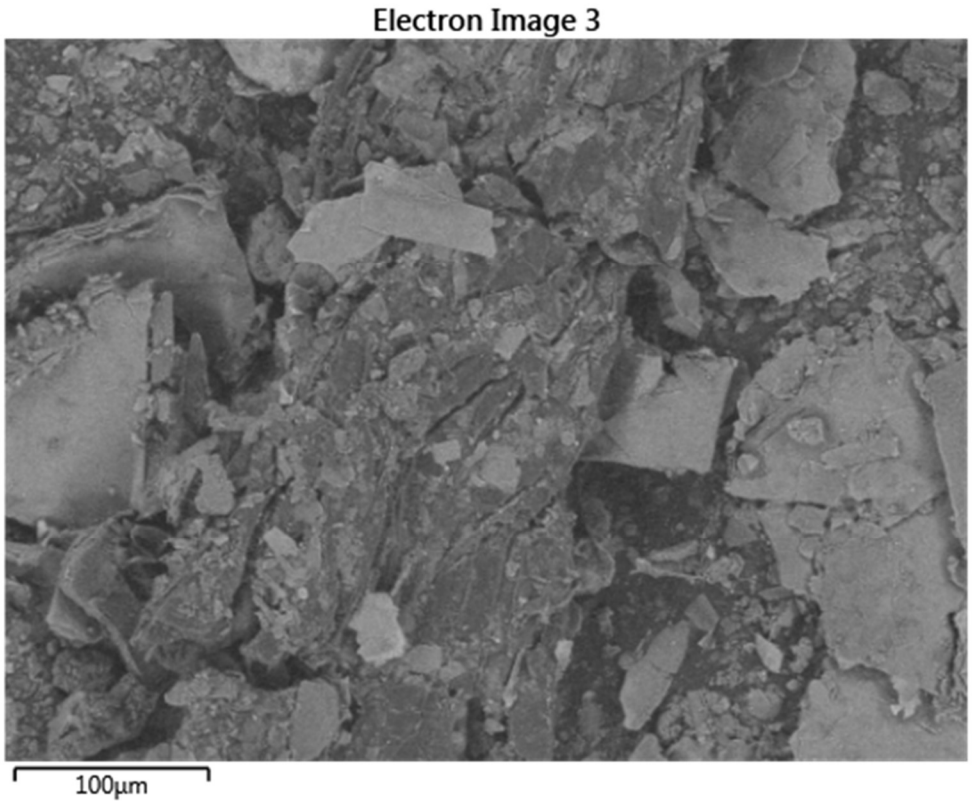

Q1-B, Maple root fiber

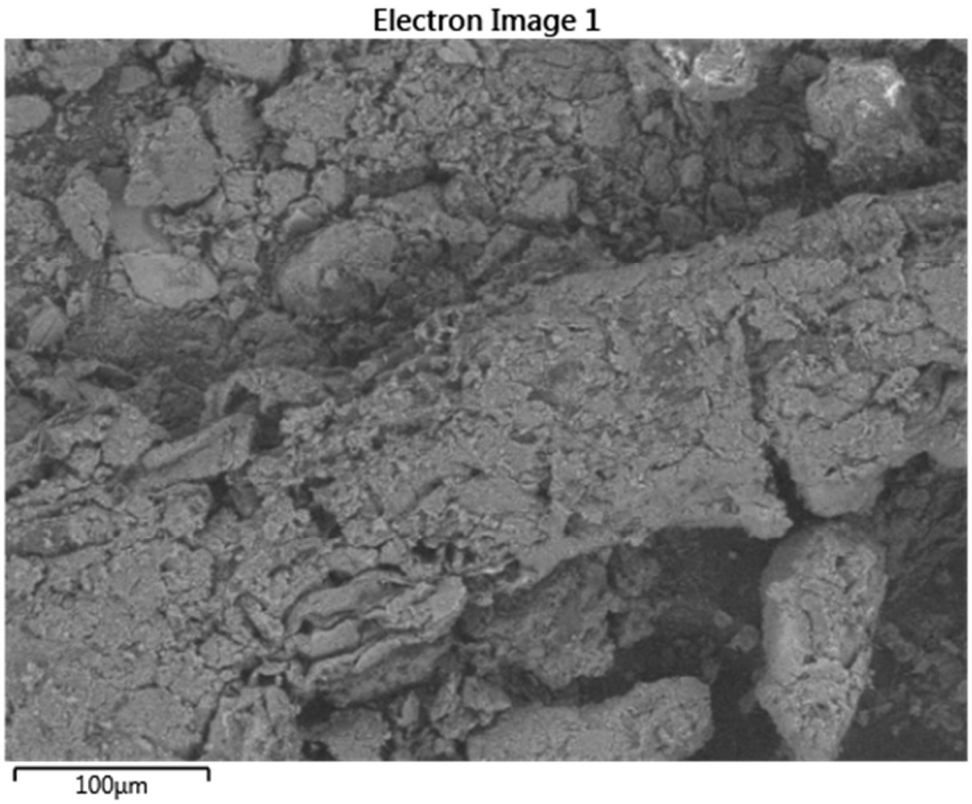

Q1-C, Maple root fiber

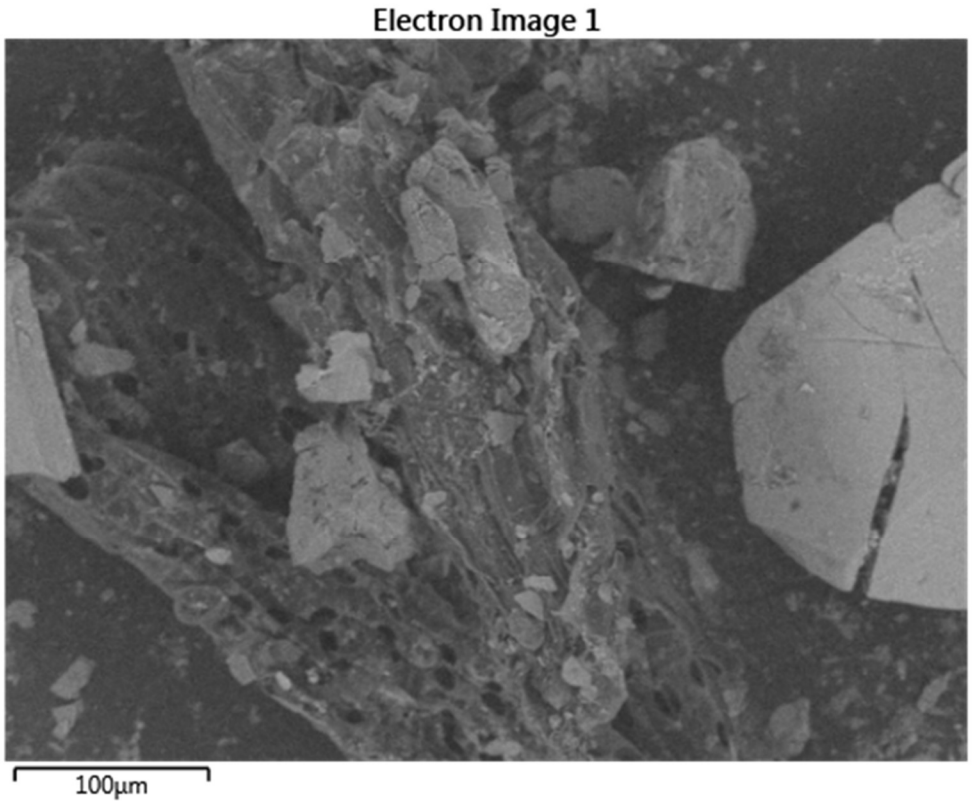

Q1-C, Pine root fiber

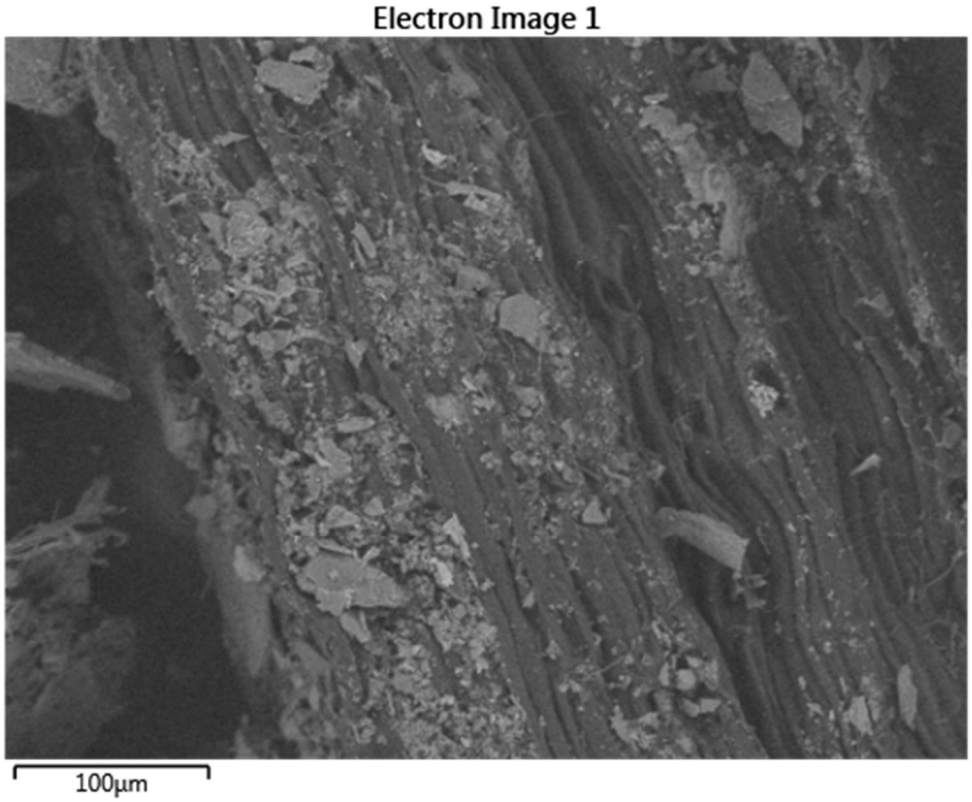

APPENDIX D: QUARRY BULK GEOCHEMISTRY

Provided below are the raw geochemistry data for bulk elemental analysis of major elements, prior to correction for 50% added silica. The data reported in Table 2 in the Discussion section are normalized assuming precisely 50% SiO_2 by weight was added.

Sample	SiO_2	Al_2O_3	Fe_2O_3	MnO	MgO	CaO	Na_2O	K_2O	TiO_2	P_2O_5	LOI	Total
Q1-B	85.12	6.95	2.69	0.018	0.13	0.08	0.16	1.05	0.321	0.02	3.36	99.9
Q1-C	83.11	7.63	2.89	0.048	0.85	1.34	1.9	1.63	0.265	0.04	0.82	100.5
Q1-R	84	7.65	1.84	0.023	0.15	0.73	1.89	2.79	0.106	0.01	0.88	100.1